Redox behaviour of cymantrene Fischer carbene complexes in designing organometallic multi-tags

Daniela I. Bezuidenhout,[a]* Belinda van der Westhuizen,[a] Pieter J. Swarts,[b] Teshica Chatturgoon,[c] Orde Q. Munro,[c]* Israel Fernández,[d]* and Jannie C. Swarts[b]*

[a] Dr D. I. Bezuidenhout, Ms B. van der Westhuizen
Chemistry Department
University of Pretoria
Private Bag X20, Hatfield 0028, Pretoria, South Africa
Tel: (+)27-12-420-2626
E-mail: daniela.bezuidenhout@up.ac.za

[b] Mr P. J. Swarts, Prof J. C. Swarts
Chemistry Department
University of the Free State
PO Box 339, Bloemfontein 9300, South Africa
Tel: (+)27-51-401-2781
E-mail: swartsjc@ufs.ac.za

[c] Ms T. Chatturgoon, Prof O. Q. Munro
School of Chemistry &Physics, University of KwaZulu-Natal
Pietermaritzburg 3209, South Africa
Tel: (+)27-33-260-5270
E-mail: munroo@ukzn.ac.za

[d] Dr I. Fernández
Departamento de Química Orgánica I, Facultad de Ciencias Químicas
Universidad Complutense de Madrid
Madrid 28040, Spain
Tel: (+)34-91-394-5155
E-mail: israel@quim.ucm.es

Abstract: A series of group 7 Fischer carbene complexes of the type $[Cp(CO)_2Mn^{I}=C(OEt)Ar]$ (Cp = cyclopentadienyl with Ar = Th = thienyl (**1a**), Fu = furyl (**2a**), or Fc = ferrocenyl (**3a**)) and biscarbene complexes $[Cp(CO)_2Mn=C(OEt)\text{-}Ar'\text{-}(OEt)C=Mn(CO)_2Cp]$ with Ar' = Th' = 2,5-thienylene (**1b**), Fu' = 2,5-furylene (**2b**) or 1,1'-ferrocendiyl (Fc') (**3b**) was synthesized and characterized. Chemical oxidation of $[Cp(CO)_2Mn=C(OEt)Fc]$ (**3a**) and isolation of the oxidised species **[3a][PF$_6$]** possessing a Mn(II) centre proved possible below –30 °C in dichloromethane solution. The ESR spectrum of the transiently stable radical cation, **[3a][PF$_6$]**, confirmed the presence of a low-spin Mn(II) centre characterized by a rhombic *g*-tensor (g_x = 1.975, g_y = 2.007, and g_z = 2.130) in frozen dichloromethane at 77 K with ^{55}Mn hyperfine coupling constants A_1, A_2, and A_3 of 115, 33, and 43 G, respectively. Electrochemical studies demonstrated the influence of the Ar substituent on the oxidation potential. All complexes showed that the redox potentials of carbene double bond reduction and Mn(I) oxidation were dependent on the type of Ar group, but only **3b** showed resolved oxidations for the two Mn(I) centres. Surprisingly, Mn(I) oxidation occurs at lower potentials than ferrocenyl oxidation. Density functional theory (DFT) calculations were carried out to delineate the nature of the species involved in the oxidation and reduction processes and clearly confirm that oxidation of Mn(I) is favoured over that of ferrocene.

Introduction

Organometallic molecular tags or labels employed to manipulate chemical and analytical properties of chemical targets mostly contain an electron-donating ferrocenyl moiety which provides a neat reversible one-electron oxidation process.[1] The anodic electrochemistry of the ferrocenyl group leads to diverse applications including

cancer therapy,[2] molecular sensors,[3] and energy transfer processes.[4] The electron-withdrawing properties and IR-active carbonyl groups of a cymantrenyl moiety, Mn(η^5-C_5H_4)$(CO)_3$,[5] make this organometallic compound an interesting and significantly different alternative as a molecular tag, although its redox chemistry has been underutilized.[6] Despite the use of cymantrenyl cathodic chemistry for immunoassays,[7] applications of cymantrenyl anodic chemistry are hitherto lacking. This dearth can be attributed not only to the high oxidation potential of the cymantrene unit (*ca*. 0.9 V vs. ferrocene) as a result of the effect of the π-accepting carbonyl groups,[8] but also to the instability of the radical cation which is still poorly understood. This paper addresses the first of these points by substituting one carbonyl ligand with a less π-accepting ligand, namely a heteroatom-substituted carbene ligand. Studies of triphenylphosphane-substituted cymantrenyl complexes showed that the thermodynamic and kinetic stabilities of the cationic complexes are greatly enhanced.[9] The effect of employing Fischer carbenes as weaker π-acceptors than carbonyls is herein imposed by synthesizing a series of cymantrene Fischer alkoxycarbene complexes containing heteroaryl (thienyl, Th, or furyl, Fu) substituents. Both the mono- and the biscarbene complexes with bridging 2,5-thienylene (Th') or 2,5-furylene (Fu') carbene substituents, were prepared. Fischer carbene complexes of the type $[(CO)_5M{=}C(X)R]$ (M = group 6 transition metal) are very well studied[10] and the electrochemical activity of these group 6 carbene complexes has recently been thoroughly investigated.[11] In contrast, examples of the group 7 type, $[Cp(CO)_2Mn{=}C(X)R]$,[12] are not as common, and reports on their redox behaviour are scarce.[13] Fine-tuning of the steric and electronic properties of the carbene moiety can be effected by modulation of the carbene substituents (X = heteroatom substituent, R = aryl substituent).[14] The introduction of a metal-containing substituent, such as ferrocenyl, opens the door for the design of organometallic multi-tag complexes. To this end, mono-and biscarbene ferrocenyl complexes were also synthesized. Electrochemical, ESR, and molecular orbital investigations of these complexes as examples of possible anodic redox multi-tags are reported herein.

Results and Discussion

Synthesis: A series of cyclopentadienyl dicarbonyl manganese carbene complexes was synthesised according to the classical procedure reported by Fischer and Maasböl.[15] Lithiation of the (hetero)arene precursors yielded a mixture of both the mono- and dilithiated (hetero)arene. The reaction mixture was reacted with 2 equivalents of $CpMn(CO)_3$ to produce the corresponding metal acylate and dimetal bisacylate complexes, which, after alkylation with Meerwein's reagent,[16] yielded both the neutral ethoxy-monocarbene and biscarbene complexes (Scheme 1).

Chemical oxidation of the Mn(I) centre of **3a** was achieved by the use of $AgPF_6$[17] (Scheme 2) to yield the radical Mn(II) species **[3a][PF_6]**. All neutral compounds were purified by column chromatography to give products as dark yellow to brown (Th, Fu) or dark red to maroon (Fc) solids. Complexes (except **2b**[18] and **[3a][PF_6]**) were stable in the absence of oxygen and could be stored for months under argon in the cold, however decomposition could be detected after 30 min in C_6D_6 and CH_2Cl_2 during electrochemical studies, but allowed enough time for electrochemical and spectroscopic studies to be completed.

Spectroscopy: By employing NMR and IR spectroscopy, electronic effects of the carbene substituents could be followed (Table 1). Both the α and ß protons in the ^{1}H NMR are deshielded as a result of π-resonance stabilization effects due to the coordination of the metal-carbene moiety. For the thienyl and ferrocenyl complexes (**1a, 1b, 3a** and **3b**) the H_α is used as a probe as it is most sensitive towards electronic ring substituent involvement. However, for furyl complexes (**2a** and **2b**) the H_γ resonances are used as a probe as these proton shifts show a more

downfield shift compared to the H_α. The assignment of the thienyl and furyl ring proton chemical shifts is based on assignments following predicted shifts for ester derivatives.[19] No usable NMR spectra could be obtained for the paramagnetic **[3a][PF$_6$]**. The expected band pattern[20] associated with the carbonyl stretches of a [CpMn(CO)$_2$L] system could be observed in the infrared spectra of all complexes, with very similar stretching frequencies (Table 1). The wavenumbers observed for complex **[3a][PF$_6$]** (Figure 1) show a significant shift of the carbonyl stretching mode bands to higher frequency, consistent with coordination to a Mn(II) ion and diminished metal-to-ligand π-back-donation due to the higher metal oxidation state and reduced d-electron density. Furthermore, the bands fall well within the expected range for the one-electron oxidation of a "piano-stool" complex. Thus, the average shift of 116 cm^{-1} from that of neutral **3a** compares favourably with that previously reported for cationic cymantrene complexes (~115 cm^{-1}).[6]

Table 1. Selected NMR and IR spectroscopic data.

Complex	H_{probe} (^{1}H NMR, ppm)[a]	$C_{carbene}$ (^{13}C NMR, ppm)[a]	IR (cm^{-1})[b]
1a	6.93	319	1936, 1872
1b	7.52	319	1948, 1896
2a	6.71	309	1942, 1876
2b	6.84	306	1935, 1886
3a	4.83	328	1938, 1862
3b	4.92	336	1927, 1858
[3a][PF$_6$]	-	-	2042, 1978

[a] Spectra recorded in C_6D_6. [b] Spectra recorded in CH_2Cl_2.

The DFT-calculated IR spectra for **3a** and **3a**$^{\bullet+}$ (Figure 1) reproduced the key carbonyl band shifts upon oxidation of **3a** in the experimental spectrum to within 11 and 16 cm^{-1} for the antisymmetric and symmetric stretching modes, respectively. Moreover, the calculated peak separation between the two CO modes for the Mn(I) complex (68 cm^{-1}, **3a**) and Mn(II) complex (70 cm^{-1}, **3a**$^{\bullet+}$) fell within 6 wavenumbers of the experimental peak separation. Note that the absolute frequencies of the calculated peaks are not expected to correlate exactly with those measured experimentally due to intrinsic limitations in the calculation method.[21] That said, a scaling factor of 0.961 for the carbonyl frequencies calculated at the HSEH1PBE/6-311+g(d,p) level of theory (in CH_2Cl_2) would bring the theoretical spectra into the correct frequency range for direct comparisons with the experimental spectra to be made. The DFT-calculated Mn(I/II) coordination geometries (Figure 1) are in excellent agreement with the X-ray data reported for the neutral and oxidized forms of the cymantrene derivative Mn(η^5-$C_5H_4NH_2$)(CO)$_3$.[6] For example, the Mn–CO distances average 1.80(1) Å in the experimental structure (the data do not allow a distinction between Mn^{I} and Mn^{II} to be made). In the simulated structures of **3a** and **3a**$^{\bullet+}$, the Mn–CO bonds contract from 1.83(1) Å to 1.77(1) Å upon oxidation of the metal. The Mn=C bond shows a similar contraction from 1.98 to 1.91 Å with the change in oxidation state of the manganese ion.

Electrochemistry: Cyclic voltammetry (CV), linear sweep voltammetry (LSV), and Osteryoung square wave voltammetry (SW) were conducted on **1 – 3**[18] in CH_2Cl_2 utilizing 0.1 mol·dm^{-3} [N(^{n}Bu)$_4$][PF$_6$] as supporting electrolyte in a glove box having oxygen and moisture levels less than 5 ppm. CV's are shown in Figures 2 and 4 while data are summarized in Table 2.

As was the case with previously reported chromium[22] and tungsten[23] Fischer ethoxycarbene complexes, [(CO)$_5$M=C(OEt)Ar] with M = Cr(0) or W(0), reduction of the Cp(CO)$_2$ Mn^{I}=C carbene double bond to a $^-$Mn^{I}-C• species is observed at low potentials (< -2.0 V vs FcH/FcH$^+$, wave I, Figure 2 and Table 2). However, in the Cr and

W systems, the metals were in the zero oxidation state. In the present series of compounds, Mn is in the +1 oxidation state. Our computational results[24] are mutually consistent with the electrochemistry in showing that this reduction is not a Mn(I) reduction to Mn(0). Figure 3 shows the computed frontier molecular orbitals of complex **2a**, where the carbene ligand adopts a vertical coordination mode and the ethoxy-group is oriented towards the carbonyl ligands (in the so-called *anti*-conformation). This conformation is reported to be the most stable conformation in similar manganese(I)-alkoxycarbene complexes.[25] The LUMO is mainly centred in the p_z atomic orbital of the carbene carbon atom. Therefore, it should be expected that the one-electron reduction process should lead to the radical anion **2a**$^{\bullet-}$ whose unpaired electron remains mainly located in the p_z orbital of the carbene carbon atom. Indeed, the computed spin density on **2a**$^{\bullet-}$ indicates a value of 0.55 e on the carbene carbon atom, thus confirming the assignment of $^{-}$Mn-C• as reduction product (Figure 3). Similar LUMO's were observed for the rest of the mono- and biscarbene complexes considered in this study.

Table 2. Cyclic voltammetry data for 0.5 mmol·dm^{-3} solutions of [Cp(CO)$_2$Mn=C(OEt)]Ar and [Cp(CO)$_2$Mn=C(OEt)-Ar'-(OEt)C=Mn(CO)$_2$Cp] complexes **1–3** in CH_2Cl_2 containing 0.1 mol·dm^{-3} [N(^{n}Bu)$_4$][PF$_6$] as supporting electrolyte at a scan rate of 100 mV s^{-1} and 20 °C. Potentials are relative to the FcH/FcH$^+$ couple.

Complex	Peaks obs.	$E^{o'}$/V, ΔE/mV	$i_p/\mu A$, i_{pc}/i_{pa}
1a Ar = Th	I (carbene)	-2.065, 76	1.60, 0.73[a]
	1 (Mn)	0.015, 73	5.82, 0.87
1b Ar' = Th' (bis derivative)	I (carbene)	-2.211, 246	18.7, 0.10[a]
	1a,b (Mn)	0.083, 214	5.82, 0.87
2a Ar = Fu	I (carbene)	-2.334, -[b]	1.44, -[b]
	1 (Mn)	0.086, 92	1.40, 0.91
	2 (OEt)	1.166, -[b]	4.12, -

The carbene double bond of **1** (Ar = Th) and **2** (Ar = Fu) is reduced at potentials at least 300 mV smaller (more negative) than the Cr(0) analogues.[22] This implies that compared to Cr^0(CO)$_5$, the CpMn^I(CO)$_2$ fragment is more electron-donating despite the metal being in the +1 oxidation state. As a consequence, the electrophilic nature of the carbene carbon atom is reduced in these group 7 Fischer carbene complexes as confirmed by the computed higher p_z occupation of the carbene carbon atom of **2a** (0.74 e) compared to its Cr(0)-carbene counterpart (0.63e), which is translated into a more difficult reduction. For Ar = Fc, reduction of the M=C double bond was only observed for the biscarbene complex **3b**. Repeated experiments with **3a** failed to show the carbene reduction within the allowed potential window of CH_2Cl_2. This finding correlates with the computed energy of the corresponding LUMO's (**3b**: –1.88 eV < **2a**: –1.83 eV < **3a**: –1.64 eV) which indicates that the reduction process should be much easier for complexes **3b** and **2a** than for **3a**, as experimentally observed (see Table 2). The spread of reduction potentials of wave I in the range $-2.334 < E^{o'} \leq -2.065$ V ($E^{o'}_{\mathbf{3a}}$ fell outside the lower limit of this range) is indicative of good electrochemical interaction between the Ar = Fu, Th or Fc group and the Mn^I=C moieties in **1–3**.

Free ferrocene and cymantrene each display a one-electron oxidation with $E^{o'} = \frac{1}{2}(E_{pa} + E_{pc})$ of cymantrene 0.92 V vs. FcH/FcH$^+$;[6] electrochemical and chemical reversibility of the cymantrenyl moiety is not as good as with

the ferrocenyl fragment.[6,17,26,27] Electrochemical reversibility is associated with $\Delta E = E_{pa} - E_{pc} = 59$ mV and $i_{pc}/i_{pa} = 1$.[27] Surprisingly, in the present carbene derivatised cymantrene series of compounds, Mn oxidation was found to occur at potentials comparable to free ferrocene. In particular, for **3a** and **3b**, results from the present electrochemical, computational and ESR study (see below) were mutually consistent in showing that Mn^{I} is oxidised *before* Ar = ferrocenyl at wave 1 in the potential range $-0.106 < E^{o'} < 0.086$V. For the biscarbene complex $[Cp(CO)_2Mn{=}C(OEt)\text{-}Ar'\text{-}(OEt)C{=}Mn(CO)_2Cp]$, Ar'= Fc', relaying of the electrostatic effects of the mixed-valent intermediate $[Cp(CO)_2Mn^{II}{=}C(OEt)\text{-}Ar'\text{-}(OEt)C{=}Mn^{I}(CO)_2Cp]$ manifested in the splitting of the oxidation peak in two components, waves 1a and 1b in Figure 2.

The above described results show that the present cymantrene-carbene derivatives behave very different compared to the previously studied group 6 $Cr^0(CO)_5$ and $W^0(CO)_5$ Fischer carbene complexes. Differences in $[L^1L^2M{=}C(OEt)\text{-}Ar]$ complexes (and by implication also the biscarbene analogues) may be summarised as follows:

a) For $L^1L^2M = (CO)_5Cr^0$, Cr(0) is first oxidised electrochemically reversibly to Cr(I) at $E^{o'} = 0.29$ V, then Ar = Fc is oxidised electrochemically reversibly to Fc^+ at $E^{o'} = 0.70$ V and finally Cr(I) is oxidised electrochemically irreversibly to Cr(II) at $E^{o'} > 1.15$ V. For Ar = Fu or Th chromium carbene analogues, the irreversible $Cr^{I/II}$ couple is between 0.95 and 1.15 V (See Figure S1).[20]

b) For $L^1L^2M = (CO)_5W^0$, Ar = Fc is first oxidised electrochemically reversibly (see Figure S1) to Fc^+ at $E^{o'} = 0.29$ - 0.31 V depending on what electrolyte is used. W(0) is irreversibly oxidised to W(II) at $E_{pa} = 1.11$ V in two overlapping one-electron transfer steps in the presence of $[N(^nBu)_4][B(C_6F_5)_4]$ as supporting electrolyte, but to W(III) in three near-overlapping one-electron transfer steps at 0.81 V in the presence of $[N(^nBu)_4][PF_6]$ as supporting electrolyte.[23]

c) For $L^1L^2M = Cp(CO)_2Mn^{I}$, compound **3a**, Mn(I) is first oxidised electrochemically reversibly to Mn(II) at $E^{o'} = -0.106$ V ($\Delta E = 96$ mV), and then Ar = Fc is oxidised electrochemically reversibly to Fc^+ at $E^{o'} = 0.442$ V ($\Delta E = 92$ mV, Table 2). Although strictly speaking $\Delta E = 59$ mV is diagnostic of electrochemical reversibility,[28] electrochemical reversible redox processes of the ferrocenyl group is universally accepted. Since ΔE for the Fc and Mn redox processes are for all practical purposes identical, we conclude that electrochemical reversibility of the cymantrenyl group is comparable with that of a ferrocenyl group in the present series of group 7 Fisher carbene complexes.

d) Only complex **2a** (Ar = Fu) showed an additional oxidative process at $E_{pa} = 1.166$ V. In analogy to the $Cr^{I/II}$ and $W^{0/III}$ couples, we believe that this may be an irreversible $Mn^{II/III}$ couple. However, all other complexes failed to show this redox process within the potential window of the solvent.

e) In terms of chemical reversibility, carbene reduction was almost irreversible with i_{pa}/i_{pc} very small (0 – 0.73; Table 2), but Mn(I) reductions was better than 85 % reversible and in some cases approached 93 % (Table 2). Interestingly though, on LSV time scale, the ferrocenyl complexes showed the oxidised species $[Cp(OC)_2Mn^{II}{=}C(OEt)(Fc^+)]$, $\mathbf{3a^{2+}}$, began to decompose notably before the LSV experiment is completed (Figure 4).

f) Wave Fc for **3b**, $[Cp(CO)_2Mn^{I}{=}C(OEt)\text{-}Fc'\text{-}(OEt)C{=}Mn^{I}(CO)_2Cp]$, does not exhibit the usual ideal CV shape. The cathodic peak is much sharper than expected. A similar observation was made for $[(CO)_5Cr{=}C(OEt)\text{-}Fc'\text{-}(OEt)C{=}Cr(CO)_5]$[22] but i_{pc}/i_{pa} for the manganese derivative was better (1.38 versus >10). The unusually large i_{pc} value for wave Fc in **3b** is attributed to electrode deposition of $\mathbf{3b^{3+}}$, the fully oxidised product (Scheme 3) onto the active surface of the electrode.

Scheme 3 highlights the proposed electrochemical pathway of the observed redox processes of **3b**. The other ethoxybiscarbene complexes undergo essentially the same processes although wave 1 is not resolved into two separate one-electron transfer processes, and the ferrocenyl wave is absent.

DFT simulations—redox chemistry: In order to gain more insight into the oxidation processes and the nature of the species involved, a Density Functional Theory (DFT) study was carried out.[24] We first focused on the oxidation process of complex **2a**. As depicted in Figure 3, the HOMO of **2a** (i.e. the orbital from which the electron is released) is mainly located on a doubly occupied *d* atomic orbital of the manganese atom. This orbital nicely represents the π-backdonation of the transition metal to the vacant p_z atomic orbital of the carbene carbon atom. Therefore, the one-electron oxidation should lead to a radical cation where the unpaired electron is mainly located at the manganese. The computed spin density on $\mathbf{2a}^{\bullet+}$ indicates a value of 1.21e on the transition metal atom thus confirming the assignment of $Cp(CO)_2Mn^{II\bullet}$=C(OEt)Fu as oxidation product (Figure 5a).

The second oxidation process was tentatively assigned to the formation of the corresponding Mn(III) dication $\mathbf{2a}^{2+}$ (see above). Our calculations nicely agree with this assignment and reveals that the dication $\mathbf{2a}^{2+}$ presents a peculiar bonding situation which is markedly different to the structures of **2a** and the radical cation $\mathbf{2a}^{\bullet+}$. As a consequence of the oxidation process which eliminates the two electrons of the HOMO of **2a** (located at the manganese), the transition metal is prone to accept more electron density from the carbene ligand. Indeed, a clear C-H agostic interaction is present in $\mathbf{2a}^{2+}$ as confirmed by the computed short Mn···HC distance of 1.919 Å (Figure 5a). Additionally, the Atoms in Molecules (AIM) method further supports the existence of this agostic interaction. As seen in Figure 5b, the Laplacian distribution of $\mathbf{2a}^{2+}$ in the Mn-H-C plane clearly reveals the occurrence of a bond critical point located between the transition metal and the hydrogen atom, which is associated with a bond path running between these two atoms. Moreover, the computed value of 0.038 e $Å^{-3}$ for the electron density at the bond critical point is in the range expected for CH agostic interactions.[28] The bonding situation of $\mathbf{2a}^{2+}$ resembles that found for related pentacarbonylchromium(0) and tungsten(0) carbene complexes formed upon 2-electron oxidation of the transition metal,[22,22] which indicates that this bonding situation seems to be general for oxidized Fischer carbene complexes regardless of the transition metal and associated ligands.

We then considered the oxidation processes of the ferrocenyl substituted carbene complexes **3a** and **3b**. Analogously to **2a**, the one-electron oxidation of **3a** leads to the formation of the radical cation $\mathbf{3a}^{\bullet+}$ whose unpaired electron is mainly located at the manganese (computed spin density of 1.21 e). This result confirms the above electrochemical conclusion that the manganese is oxidized before the iron atom and is consistent with the ESR spectrum of $\mathbf{3a}^{\bullet+}$. Subsequent one-electron oxidation may lead to two different species, namely the open-shell singlet complex formed upon oxidation of the Fe(II) to Fe(III) or, alternatively, the closed-shell singlet involving the oxidation of the Mn(II) to Mn(III). Our calculations reveal that the former species is 26.4 kcal/mol more stable than the latter, thus suggesting that the dication $\mathbf{3a}^{+2}$ presents two unpaired electrons (computed spin densities of –1.26 and 1.30 for Mn and Fe, respectively, see Figure 6a).

A similar behaviour can be found in biscarbene complexes **3b**. As readily seen in Figure 6b, the first one-electron oxidation involves the Mn(I) to Mn(II) reaction to produce the radical cation $\mathbf{3b}^{\bullet+}$. This process is followed by the oxidation of the other manganese centre to produce the open-shell singlet $\mathbf{3b}^{+2}$. Finally, the Fe(II) to Fe(III) oxidation occurs to form complex $\mathbf{3b}^{\bullet+3}$ in which each metal bears an unpaired electron. Therefore, our calculations fully support the electrochemical pathway proposed in Scheme 3.

ESR spectroscopy: Lastly, we carried out an ESR analysis of the chemically oxidised product **[3a][PF_6]** to

experimentally support the above computational assignment of the radical cation as a $Cp(CO)_2Mn^{II}\bullet$–C species. Briefly, **[3a][PF$_6$]** was generated by $AgPF_6$-mediated oxidation of **3a** at –41 °C in CH_2Cl_2 (Scheme 2); transfer of the solution to a gas-tight ESR tube after 7 min followed by immediately recording the X-band ESR spectrum at 77 K permitted observation of a clean spectrum of the transiently stable radical cation (Figure 7). (Note that a sample removed from the reaction vessel after 35 min afforded only a low-resolution, low-intensity ESR spectrum indicative of time-dependent decay of **[3a][PF$_6$]** to one or more ESR-silent species in solution.) The ESR spectrum of **3a**$^{\bullet+}$ is characterized by a rhombic *g*-tensor with the components g_z = 2.130, g_y = 2.007, and g_x = 1.975. Each *g*-component is, furthermore, split into six lines as a result of hyperfine coupling to the ^{55}Mn nucleus (I = 5/2, 100%). While the hyperfine coupling clearly confirms oxidation of Mn(I) (diamagnetic low-spin d^6) to Mn(II) (S = ½ d^5), the ensuing peak overlap significantly complicates interpretation of the derivative spectrum and creates difficulties not only when attempting to locate the *g*-tensor components, but also when attempting to delineate the hyperfine coupling constants (*A*-values). We found that deconvolution of the ESR absorption spectrum (Figure 7a) into a summation of Voigt functions[30] partly simplified the task of locating the *g*-tensor components and measuring the hyperfine coupling constants from the experimental spectrum. As is customary in spectroscopy,[30] we chose to fit the data with a summation of Voigt functions as these functions represent a convolution of Gaussian and Lorentzian line shapes, have a sound theoretical basis, and are well-suited to analysing spectroscopic absorption bands in which both lifetime broadening (e.g. due to spin-lattice relaxation) as well as Doppler, instrumental, and proximity line broadening are present to varying extents. This requires that the derivative ESR spectrum be fit in its integrated form (i.e. absorption spectrum, Figure 7a). In systems with rhombic *g*-tensors and no hyperfine coupling [e.g. low-spin Fe(III)] spectral deconvolution of the absorption trace is straightforward; the situation is, however, more complex in the case of low-spin Mn(II) due to each *g*-tensor component affording six absorption lines.

Given the above limitations expected for spectral deconvolution of the ESR absorption spectrum of a low-spin Mn(II) ion, precise location of g_y is nevertheless straightforward and simply achieved using H_{max} for the most intense component peak (3352 G) in the absorption spectrum (Figure 7a). Location of g_x and g_z is more difficult especially since the Voigt functions themselves are of variable band width and, in some cases, represent more than one overlapped peak. For g_z, the position of this tensor component is expected to be at the centre of gravity of the six independent equal-intensity lines into which the signal splits by virtue of hyperfine coupling to ^{55}Mn. Only the three low-field hyperfine lines are in fact easily discerned. That said, the experimental anisotropic hyperfine coupling constant A_1 (115 G) may be used to locate g_z since it is at precisely 2.5A_1 to higher magnetic field from the lowest-field line in the spectrum. Unfortunately locating g_x is significantly more problematic. Our best estimate using an analysis of the Voigt components in conjunction with the value of A_3 measured as indicated in Figure 7b places g_x at 3428 G (i.e., g_x = 1.975). From the Voigt functions in Figure 7a, the anisotropic hyperfine coupling constants A_2 and A_3 measure 33 and 43 G, respectively. Note that measurement of A_3 from either the absorption or derivative spectrum is complicated somewhat by the fact that the peak expected between the indicted pair of lines is unresolved (as a result of overlap). (The spacing 2A_3 is, however, well-resolved and simple to measure.)

While useful, peak deconvolution of the ESR absorption spectrum is subject to significant uncertainty, particularly in the lower magnetic field range, contingent upon the lower intensity of the spectral envelope. The estimate of A_1 in Figure 7a [82(23) G] is therefore the least accurate of the three hyperefine coupling constants—in contrast to the situation when analyzing the first derivative of the spectral envelope. We therefore feel that for **[3a][PF$_6$]** it is not only practically sound, but indeed preferable, to use the value of A_1 determined from analysis of the derivative trace (i.e. A_1 = 115 G, Figure 7b).

A key question that emerged during analysis of the ESR spectrum of **[3a][PF$_6$]** concerned assignment of the *g*-

tensor components as g_x, g_y, or g_z. Experimental assignment of the *g*-tensor components requires determination of the tensor axes relative to the molecular framework, which requires a large face-indexed crystal, the X-ray crystal structure, and analysis of the ESR spectrum as a function of the orientation of the crystal in the applied magnetic field. In the absence of a suitable single crystal, we resorted to calculating the *g*-tensor and anisotropic spin-dipole couplings for **3a**$^{\bullet+}$ using a suitable hybrid DFT functional and several basis sets both *in vacuo* and in a CH_2Cl_2 solvent continuum. The *g*-values calculated with the all-electron basis set 6- 311g(d,p)[31] (Table 3) are remarkably independent of the presence or absence of diffuse functions or solvent and are in excellent agreement with the experimental values. Furthermore, the calculated *g*-shifts relative to the free electron *g*-value allow unambiguous assignment of the experimental *g*-values as depicted in Figure 7b. The *g*-values calculated using the effective core potential (ECP) basis set SDD[32] are also in good agreement with the experimental values; only g_z deviates by more than 20,000 ppm from the experimental value. Because of the generally good precision in the simulation data we can determine the mean calculated *g*-values using all of the available data for **3a**$^{\bullet+}$: g_x = 1.998(1), g_y = 2.03(1), and g_z = 2.13(5).

Table 3. DFT-calculated parameters for **3a**$^{\bullet+}$ as a function of basis set type.[a]

	6-311+g(d,p) DCM PCM	6-311+g(d,p)	6-311g(d,p)	SDD
g-tensor x-shift	–4632.9	–5018	–4510.8	–2850
g-tensor y-shift	31090.6	31140	33090.8	9549.2
g-tensor z-shift	149600.2	151317.5	148546.9	57350
g_x calc.	1.998	1.997	1.998	1.999
g_y calc.	2.033	2.033	2.035	2.012
g_z calc.	2.152	2.154	2.151	2.060
g_{iso} calc.	2.061	2.061	2.061	2.024
Spin density	1.17	1.09	1.14	1.29
IFCC / G	–40.28	–41.33	–40.07	–0.01
A_1 / G	–71.104	–77.409	–76.83	–75.29
A_2 / G	22.278	36.133	30.636	35.728
A_3 / G	48.826	41.276	46.194	39.565
4s	0.357	0.353	0.346	0.318
4px	0.348	0.329	0.021	0.317
4py	0.356	0.342	0.024	0.324

[a] Units and abbreviations: DCM PCM, dichloromethane polarization continuum model; *g*-shifts relative to g_e for the free electron are in ppm; spin (Mulliken) and electron densities (NBO 3.0[33]) are given in electron charge units and are listed for the Mn(II) ion only; IFCC, isotropic Fermi contact coupling for Mn; A_n are the anisotropic spin-dipole coupling constants for Mn (where *n* is the principal axis system component).

The unpaired spin densities on the Mn(II) ion of **3a**$^{\bullet+}$ range from 1.09–1.29 e depending on the basis set used and are consistent with the value of 1.21 e calculated at the B3LYP/def2-SVP level of theory (*vide supra*). The calculated anisotropic spin-dipole couplings in Table 3 vary somewhat more with the basis set and/or the presence of solvent. The mean calculated anisotropic spin-dipole coupling constants are: A_1 = –75(3) G, A_2 = 31(6) G, and A_3 = 44(4) G. From the experimental ESR spectrum of **3a**$^{\bullet+}$, we were able to reliably measure A_2 (33 G) and A_3 (43 G), but not A_1. The value of A_1 determined from the derivative trace (115 G) clearly deviates significantly from the calculated value of A_1. That said, determination of A_1 from the Voigt functions below 3150 G in Figure 7a yields an estimated mean A_1 value of 82(23) G—somewhat closer to the DFT-calculated value, but subject to substantial uncertainty. Significantly, the relative absolute magnitudes of the experimental and DFT-calculated hyperfine coupling constants follow the same order ($A_2 < A_3 << |A_1|$), which affirms the approach we have used for assignment of the experimental ESR spectrum of **[3a][PF$_6$]**.

Importantly, replacement of one of the three CO ligands in cymantrene, Mn(Cp)(CO)$_3$, with a carbene ligand in the present case of **3a**$^{\bullet+}$ lowers the symmetry of the *g*-tensor from tetragonal to rhombic. A switch in the *g*-tensor anisotropy may thus be used to detect the substitution of a carbonyl ligand in Mn(II) cymantrene derivatives (at least for carbenes). With the exception of the rhombic *g*-tensor, the magnitudes of the key ESR spectral parameters for **3a**$^{\bullet+}$ are broadly in accord with the tetragonal *g*- and *A*-tensor components reported previously for Mn(Cp$^{\gamma}$)(CO)$_3$ derivatives, where γ is a substituent on the Cp ligand.[6] These latter tricarbonyl complexes have *g*- and *A*-values in the following ranges: $g_{\|} \sim 2.12–2.21$, $g_{\perp} \sim 2.01–2.08$, $A_{\|} \sim 65–79$ G, and $A_{\perp} \sim 30–50$ G.[6]

Conclusion

Mono- and biscarbene cymantrene derivatives [Cp(CO)$_2$Mn^{I}=C(OEt)Ar] **1a** (Ar = Th), **2a** (Ar = Fu), **3a** (Ar = Fc) and [Cp(CO)$_2$Mn^{I}=C(OEt)-Ar'-(OEt)C=Mn^{I}(CO)$_2$Cp] with Ar' = Th' (**1b)**, Ar' = Fu' (**2b)** and Ar' = Fc' (**1b)** were prepared via the classical Fischer route. Low-temperature chemical oxidation of **3a** with $AgPF_6$ permitted isolation of transiently stable [Cp(CO)$_2$Mn^{II}=C(OEt)Fc][PF$_6$], **[3a][PF$_6$]**. From an FTIR study, the > 110 cm^{-1} shift of the carbonyl stretching frequencies for **[3a][PF$_6$]** relative to neutral **3a** indicates that the oxidation is that of the metal carbonyl moiety, as opposed to Fe^{II}/Fe^{III} oxidation of the ferrocenyl substituent. An electrochemical study on **1**–**3** confirmed that Mn(I) is oxidized before the ferrocenyl group, and that both these oxidations involve one-electron transfer processes. Complex **3b** showed clear splitting of the Mn(I) oxidation into "a" and "b" components but **1b** and **2b** did not. This is consistent with Ar' = Fc' being more effective in transmitting electrostatic interactions between cymantrenyl moieties than Ar' = Fu' or Th'. Poorly chemically reversible reduction of Mn=C to $^{-}$Mn^{I}-C• was observed at far negative potentials (< –2.065 V vs. FcH/FcH^{+}). DFT calculations showed that the mono- and biscarbene complexes containing one or two Mn(I) ions always undergo one-electron oxidation of manganese before the onset of ligand or ferrocene oxidation. This reflects localization of the HOMO on the Mn=C group of the cymantrene unit. Our interpretation of the electrochemical and DFT data was tested experimentally using ESR spectroscopy to probe **3a**$^{\bullet+}$ produced by direct chemical oxidation of **3a**. The ESR spectrum revealed a rhombic *g*-tensor for an S = ½ Mn(II) ion with ^{55}Mn hyperfine coupling constants in accord with those observed for [Mn(Cp$^{\gamma}$)(CO)$_3$]$^{+}$ derivatives. The rhombic *g*-tensor for **3a**$^{\bullet+}$ evidently reflects reduced symmetry at the metal centre consistent with replacement of one cymantrene CO ligand by the Mn=C(OEt)Fc carbene moiety.

Experimental Section

General: All operations were carried out under an inert atmosphere of nitrogen or argon gas using standard Schlenk techniques. Solvents were dried by refluxing on sodium metal (hexane, tetrahydrofuran and diethylether) or over phosphorous pentoxide (CH_2Cl_2) and then distilled under nitrogen prior to use. Chemicals were used

without further purification unless stated otherwise. Triethyloxonium tetrafluoroborate (Et_3OBF_4) was synthesized according to literature procedures.[16] Purification with column chromatography was done using silica gel 60 (0.0063–0.200 mm) as stationary phase. A Bruker AVANCE 500 spectrometer was used for NMR recordings. ^{1}H NMR spectra were recorded at 500.139 MHz and ^{13}C NMR spectra at 125.75 MHz. The signal of the solvent was used as reference: ^{1}H $CDCl_3$ at 7.24 ppm; C_6D_6 at 7.16 ppm and ^{13}C CDCl3 at 77.00 ppm; C_6D_6 at 128.06 ppm. IR spectra were recorded on a Perkin-Elmer Spectrum RXI FT-IR spectrophotometer in CH_2Cl_2 as solvent. Only the vibrational bands in the carbonyl-stretching region (ca. 1600–2200 cm^{-1}) were recorded.

Synthesis: Synthesis and characterization of **1b**,[12c] **3a**[12b] and **3b**[12b] have been reported earlier. Novel complexes **1a**, **2a** and **2b** were prepared in an adapted version of a previously reported method.[24]

*Synthesis of [Cp(CO)$_2$Mn=C(OEt)Th] (**1a**) and [Cp(CO)$_2$Mn=C(OEt)Th'(OEt)C=Mn(CO)$_2$Cp] (**1b**).*

2-Bromothiophene (2 mmol, 0.2 mL) was dissolved in 30 mL thf and cooled to -70^{o}C. One equivalent LDA (2 mmol) was added and the solution stirred for 15 minutes at low temperature. $CpMn(CO)_3$ (2 mmol, 0.40 g) was added in one portion and stirred for 15 minutes after which the cold bath was removed and the mixture allowed to stir for an additional 1hr. The reaction mixture was then cooled to –60 ^{o}C and nBuLi (1.5 M, 2 mmol, 1.3 mL) was slowly added. After 30 minutes another equivalent of $CpMn(CO)_3$ (2 mmol, 0.40 g) was added and allowed to stir for 15 min in the cold. The bath was removed and the mixture stirred for 1 hr at room temperature. The solvent was changed to CH_2Cl_2 and the reaction cooled to –40 ^{o}C after which 2 equivalents of Et_3OBF_4 with 10% excess (4.4 mmol) dissolved in CH_2Cl_2 was added. After 15 min in the cold bath the mixture was allowed to reach room temperature over an hour. Purification with column chromatography on silica and gradient elution starting with 1:4 CH_2Cl_2/hexane solution afforded the ochre coloured monocarbene (**1a**) and the maroon coloured biscarbene (**1b**) complexes.

For **1a**: Yield 45% (0.28g), dark yellow crystals. Anal. calcd. for $MnC_{14}H_{13}O_3S$ (316.28), C:53.16, H:4.15; Found C:53.18, H:4.16. ^{1}H NMR (C_6D_6, δ/ppm): 7.80 (br, 1H, Th-H_α), 6.93 (br, 1H, Th-H_γ), 6.96 (br, 1H, Th-$H_ß$), 4.75 (br, 2H, C**H$_2$**), 4.14 (br, 5H, **Cp**), 1.19 (br, 3H, C**H$_3$**); ^{13}C NMR (C_6D_6, δ/ppm): 319.46 ($C_{carbene}$), 231.19 (CO), 156.74 (Th_{ipso}), 136.60 (Th-C_γ), 136.30 (Th-C_α), 130.78 (Th-$C_ß$), 83.97 (Cp), 73.99 (CH_2), 15.11 (CH_3). IR (CH_2Cl_2, ν(CO)/cm^{-1}): 1936, 1872.

*Synthesis of [Cp(CO)$_2$Mn=C(OEt)Fu] (**2a**) and [Cp(CO)$_2$Mn=C(OEt)Fu'(OEt)C=Mn(CO)$_2$Cp] (**2b**)*

Furan (2.7 mmol, 0.2 mL) was dissolved in 50 mL thf and cooled to –20 ^{o}C. nBuLi (1.5 M, 1.8 mL) was added slowly to the stirring solution which was then left to react in the cold for 30 min. It was then cooled further to –40 ^{o}C and $CpMn(CO)_3$ (2.7 mmol, 0.55 g) was added in one portion. The cold bath was removed after 15 min and the mixture left to stir at room temperature for 1 hr. The reaction was cooled again to –78 ^{o}C and LDA (0.18 M, 15 mL) was added and the reaction stirred for 1 hr. It was warmed to –40 ^{o}C and $CpMn(CO)_3$ (2.7 mmol, 0.55 g) was added. After stirring for 1 hr at room temperature the acylate was quenched with Et_3OBF_4 (0.54 M, 12 mL) at –20 ^{o}C in CH_2Cl_2 and stirred for another hour at room temperature. Purification was performed by column chromatography on silica and gradient elution starting with 1:4 CH_2Cl_2/hexane solution. The brown coloured monocarbene (**2a**) and the maroon coloured biscarbene (**2b**) complexes were collected.

For **2a**: Yield 56% (0.48g), dark yellow crystals. Anal. calcd. for $MnC_{14}H_{13}O_4$ (316.21), C:53.16, H:4.15; Found C:53.21, H:4.20. ^{1}H NMR (C_6D_6, δ/ppm): 6.71 (br, 2H, Fu-H_γ), 6.71 (br, 1H, Fu-H_α), 5.97 (br, 1H, Fu-$H_ß$), 4.75 (br, 2H, C**H$_2$**), 4.38 (br, 5H, **Cp**), 1.21 (br, 3H, C**H$_3$**); ^{13}C NMR (C_6D_6, δ/ppm): 309.31 ($C_{carbene}$), 232.22 (CO), 164.49 (Fu_{ipso}), 145.20 (Th-C_γ), 112.03 (Fu-C_α), 111.50 (Fu-$C_ß$), 84.27 (Cp), 73.20 (CH_2), 15.27 (CH_3). IR (CH_2Cl_2, ν(CO)/cm^{-1}): 1942, 1876.

For **2b**: Yield 32% (0.44g), maroon crystals. Anal. calcd. for $Mn_2C_{24}H_{22}O_8$ (548.38), C:52.56, H:4.05; Found C:52.59, H:4.07. ^{1}H NMR (C_6D_6, δ/ppm): 6.84 (br, 2H, Fu-H), 4.77 (br, 4H, C**H$_2$**), 4.41 (br, 10H, **Cp**), 1.25 (br, 6H, C**H$_3$**); ^{13}C NMR (C_6D_6, δ/ppm): 306.82 ($C_{carbene}$), 232.32 (CO), 161.57 (Fu_{ipso}), 116.57 (Fu), 85.84 (Cp), 73.35 (CH_2), 15.40 (CH_3). IR (CH_2Cl_2, ν(CO)/cm^{-1}): 1935, 1886.

*Synthesis of [Cp(CO)$_2$Mn=C(OEt)Fc][PF$_6$] (**[3a]PF$_6$**).*

Compound **3a** (0.006g, 0.01 mmol) was dissolved in CH_2Cl_2 and cooled to –35 °C. $AgPF_6$ (0.003g, 0.01 mmol) was added in one portion after which the colour changed rapidly from dark red to brown. The solution was filtered using cannula filtration.

For **[3a][PF$_6$]**: Yield 78% (0.006g), dark brown salt. IR (CH_2Cl_2, ν(CO)/cm^{-1}): 2042, 1978.

Electrochemistry: Cyclic voltammograms (CV's), square wave voltammograms (SW's) and linear sweep voltammograms (LSV's) were recorded on a Princeton Applied Research PARSTAT 2273 voltammograph running PowerSuite (Version 2.58). All experiments were performed in a dry three-electrode cell. A platinum wire was used as auxiliary electrode while a glassy carbon working electrode (surface area 3.14 mm^2) was utilized after polishing on a Buhler polishing mat first with 1 micron and then with 1/4 micron diamond paste. A silver wire was used as pseudo internal reference under an argon atmosphere inside an M Braun Lab Master SP glovebox filled with high purity argon (H_2O and O_2 < 5 ppm). All electrode potentials are reported using the potential of the ferrocene/ferrocenium redox couple [FcH/FcH$^+$] (FcH = (η^5-C_5H_5)$_2$Fe, E°′ = 0.00 V) as reference.[34] However, decamethyl ferrocene, Fc*, was used as internal standard to prevent signal overlap with the ferrocenyl of **3**. Decamethylferrocene has a potential of −550 mV versus free ferrocene with ΔE = 72 mV and i_{pc}/i_{pa} = 0.99 under the conditions employed.[26] Analyte solutions (0.5 mmol dm^{-3}) were prepared in dry CH_2Cl_2 in the presence of 0.1 mol dm^{-3} [(^{n}Bu$_4$)N][PF_6]. Analyses were performed at 20 °C. Data were exported to a spread sheet program for manipulation and diagram preparation.

ESR Spectroscopy: The cation radical **[3a][PF$_6$]** was generated as follows for ESR spectroscopy. Solid compound **3a** (0.060 g, 0.10 mmol) and solid $AgPF_6$ (0.030 g, 0.10 mmol) were placed together in a dry Schlenk tube under nitrogen at –41 °C in an acetonitrile/liquid nitrogen slush bath. After thermal equilibration, 10 mL of dry CH_2Cl_2 that had been pre-cooled to –41 °C was added to the solids via cannula transfer from a reservoir flask under nitrogen. The solution immediately changed from orange-brown to deep red and was mixed by swirling for *ca*. 6 min at –41 °C before transferring a *ca*. 600-µL aliquot of the reaction mixture by cannula filtration into a gas-tight ESR tube suspended in the slush bath at –41 °C. The sample aliquot was immediately flash-frozen in liquid nitrogen and then transferred to a liquid nitrogen-containing quartz finger dewar mounted in the sample slot of the microwave resonator of a Bruker EMX-plus X-band ESR spectrometer operating at a frequency of 9.421260 GHz. The final spectrum was obtained from 12 scans over the spectral range 2700–3900 G using the data acquisition parameters indicated in Figure 7. The spectral data in derivative mode were first filtered (boxcar averaging with a 7 point window and 9th order polynomial filter) and then resolution-enhanced (line-broadening

function = 0.200 G) for the final plot. The ESR absorption spectrum (raw data) was deconvoluted into a series of constituent Voigt functions using FitYk 0.9.8[35] in order to facilitate *g*-value assignments. The fit parameters are given in the Supporting Information.

Molecular simulations: Geometry optimizations without symmetry constraints were carried out using the Gaussian09 suite of programs.[36] Electron correlation was partially taken into account using the hybrid functional denoted as B3LYP (and uB3LYP for radical cations and open-shell species)[37] in combination with double-ζ quality plus polarization def2-SVP[38] basis set for all atoms (this level is denoted B3LYP/def2-SVP). Calculation of the vibrational frequencies[39] at the optimized geometries showed that the compounds are minima on the potential energy surface. The AIM[40] results described in this work correspond to calculations performed at the B3LYP/def2-SVP level on the optimized geometry of **2a**$^{+2}$. The topology of the electron density was studied using the AIMAll program package.[41] DFT simulations for analysis of the ESR spectrum of **3a**$^{\bullet+}$, specifically determination of the *g*- and *A*-tensors, were performed with an unrestricted wave function using the full Heyd-Scuseria-Ernzerhof hybrid functional HSEH1PBE[42] and three basis sets: the effective core potential basis set SDD[32] and the all-electron basis sets 6-311g(d,p)[31] or 6-311+g(d,p). We also determined the electronic structure of **3a**$^{\bullet+}$ in CH_2Cl_2 (polarization continuum model, PCM). The geometries of all structures were fully optimized; no negative eigenvalues were calculated in any of the post-optimization frequency jobs.

Acknowledgements

This work is supported by the National Research Foundation (NRF) of South Africa, (D.I.B., Grant number 76226; J.C.S., Grant number 81829). I. F. acknowledges the Spanish MICINN and CAM (Grants CTQ2010-20714-CO2-01/BQU, Consolider-Ingenio 2010, CSD2007-00006, S2009/PPQ-1634). O.Q.M. acknowledges financial support from the University of KwaZulu-Natal and the NRF.

References

[1] a) L. Cuffe, R. D. A. Hudson, J. F. Gallagher, S. Jennings, C. J. McAdam, R. B. T. Connelly, A. R. Manning, B. H. Robinson, J. Simpson, *Organometallics*, **2005**, *24*, 2051-2060; b) S. Warren, T. McCormac, E. Dempsey, *Bioelectrochemistry*, **2005,** *67,* 23-35; c) A. D. Ryabov, *Ad. Inorg. Chem.*, **2004**, 55, 201-269; d) K. C. Kemp, E. Fourie, J. Conradie, J. C. Swarts, J. C. *Organometallics,* **2008**, *27*, 353-362; e) P. D. Beer, E. Hayes, *J. Coord. Chem.,* **2003***, 240,* 167-189*;* (f) A. Chaubey, B. D. Malhotra, *Biosens. Bioelectron.*, **2002**, *17*, 441-456.

[2] a) R. F. Shago, J. C. Swarts, E. Kreft, C. E. J. Van Rensburg, *Anticancer Res.* **2007**, *27*, 3431-3433; b) C. E. J. Van Rensburg, E. Kreft, J. C. Swarts, S. R. Dalrymple, D. M. Macdonald, M. W. Cooke, M. A. S. Aquino, *Anticancer Res*. **2002**, *22*, 889-892; c) A. Gross, N. Hüsken, J. Schur, L. Raszeja, I. Ott, N. Metzler-Nolte, *Bioconjugate Chemistry*, **2012**, *23*, 1764-1774; d) J. C. Swarts, T. G. Vosloo, S. J. Cronje, W. C. Du Plessis, C. E. J. Van Rensburg, E. Kreft, J. E. Van Lier, *Anticancer Res.* **2008**, *28*, 2781-2784; e) I. Ott, K. Kowalski, R. Gust, J. Maurer, P. Mücke, R. F. Winter, *Bioorg. Med. Chem. Lett.* **2010**, *20*, 866-869.

[3] A. R. Pike, L. C. Ryder, B. R. Horrocks, W. Clegg, B.A. Connolly, A. Houlton, *Chem. Eur. J.* **2004**, *11*, 344-353.

[4] F. Spanig, C. Kolvacs, F. Hauke, K. Ohlubo, F. Fukuzumi, D. M. Guldi, A. Hirsch, *J. Am. Chem. Soc.* **2009**, *131*, 8180-8195.

[5] a) S. D. Lepore, A. Khoram, D. C. Bromfield, P. Cohn, V. Jairaj, M. A. Silvestri, *J. Org. Chem.*, **2005**, *70*, 7443-7446; b) Z. Zhang, S. D. Lepore, *Tetrahedr. Lett.,* **2002**, *43*, 7357-7360; c) H. Gradén, N. Kann, *Curr. Org. Chem.,* **2005**, *9*, 733-763; d) L. M. Dorozhkin, V. A. Nefedov, A. G. Sabelnikov, V. G. Sevastjanov, *Sens. Actuators B.,* **2004**, *B99*, 568-570.

[6] D. R. Laws, D. Chong, K. Nash, A. L. Rheingold, W. E. Geiger, *J. Am. Chem. Soc.*, **2008**, *130*, 9859-9870.

[7] a) M. Hromadova, M. Salmain, N. Fischer-Durand, L. Pospisil, G. Jaouen, *Langmuir*, **2006**, *22*, 506-511; b) M. Hromadoca, M. Salmain, R. Sokolova, L. Pospisil, G. Jaouen, *J. Organomet. Chem.,* **2003**, *668*, 17-24.

[8] a) C. N. Field, J. C. Green, A. G. J. Moody, M. R. F. Siggel, *Chem. Phys.*, **1996**, *206*, 211-223; b) D. C. Calabro, D. L. Lichtenberger, *J. Am. Chem. Soc.*, **1981**, *103*, 6846-6852; c) D. L. Lichtenberger, R. F. Fenske, *J. Am. Chem. Soc.,* **1976**, 98, 50-63.

[9] C. G. Atwood, W. E. Geiger, T. E. Bitterwolf, *J. Electroanal. Chem.*, **1995**, *397*, 279-285.

[10] Selected recent reviews on the chemistry of group 6 Fischer carbene complexes: a) M. A. Sierra, I. Fernández, F. P. Cossío, *Chem. Commun*. **2008**, 4671; b) K. H. Dötz, J. Stendel, *Chem. Rev*. **2009**, *109*, 3227; c) J. W. Herndon, *Coord. Chem. Rev*. **2010**, *254*, 103; d) M. A. Fernández-Rodríguez, P. García-García, E. Aguilar, *Chem. Commun*. **2010**, *46*, 7670; e) I. Fernández, F. P. Cossío, M. A. Sierra, *Acc. Chem. Res*. **2011**, *44*, 479; f) D. I. Bezuidenhout, S. Lotz, D.C. Liles, B. van der Westhuizen, *Coord. Chem. Rev.*, **2012**, *256*, 479-524.

[11] a) I. Hoskovcová, R. Svěřinová, J. Roháčová, D. Dvořák, T. Tobrman, S. Záliš, J. Ludvík, *Electr. Chim. Acta,* **2011**, *56*, 6853-6859; b) I. Hoskovcová, J. Roháčová, D. Dvořák, T. Tobrman, S. Záliš, R. Svěřinová, J. Ludvík,*Electr. Chim. Acta*, **2010**, *55*, 8341-8351.

[12] a) M. Landman, W. Barnard, P. H. van Rooyen, D. C. Liles, *J. Mol. Struct.*, **2012**, *1021*, 76-83; b) D. I. Bezuidenhout, S. Lotz, M. Landman, D. C. Liles, *Inorg. Chem.*, **2011**, *50(4)*, 1521-1533; c) Y. M. Terblans, M. H. Roos, S. Lotz, *J. Organomet. Chem.*, **1998**, *566(1-2)*, 133-142; d) E. O. Fischer, V. N. Postnov, F. R. Kreissl, *J. Organomet. Chem.*, **1982**, *231(4)*, C73-C77.

[13] A related electrochemical study on an Fe-NHC complex has been reported, see: L. Mercs, G. Labat, A. Neels, A. Ehlers, M. Albrecht, *Organometallics,* **2006**, *25*, 5648-5656.

[14] D. I. Bezuidenhout, W. Barnard, B. van der Westhuizen, E. van der Watt, D. C. Liles, *Dalton Trans.*, **2011**, *40*, 6711-6721.

[15] E. O. Fischer, A. Maasböl, *Angew. Chem.Int. Ed. Engl.***1964**, *3(8)*, 580-581.

[16] H. Meerwin, *Org. Synth.*, **1966**, *46*, 113-115.

[17] N. G. Connolley, W. E. Geiger, *Chem. Rev.*, **1996**, *96*, 877-910.

[18] Compound **2b** was prepared and spectroscopically characterized. However, the instability of **2b** with regards to atmospheric decomposition precluded it from the electrochemical studies, and no usable CV could be recorded.

[19] a) S. Lotz, C. Crause, A. J. Olivier, D. C. Liles, H. Gorls, M. Landman, D. I. Bezuidenhout, *Dalton Trans.* **2009**, 697−710; b) M. Landman, J. Ramontja, M van Staden, D. I. Bezuidenhout, P. H. van Rooyen, D. C. Liles, S. Lotz, *Inorg. Chim. Acta* **2010**, *363*, 705−717; c) G. M. Chu, I. Fernández, M. A. Sierra, *Chem. Eur. J.* **2013**, *19*, 5899−5908; d) E. Pretch, J. Seibl, T. Clerc, W. Simon, *Tables for Spectral Data for Structure Determination of Organic Compounds*, 2nd ed.; Springer-Verlag: Berlin, Germany, 1989.

[20] a) P. S. Braterman, Metal Carbonyl Spectra, Academic Press Inc., London, **1975**, p. 68; b) D. M. Adams, *Metal–Ligand and Related Vibrations*, Edward Arnold Publishers Ltd, London, 1967, p. 98.

[21] I. M. Alecu, J. Zheng, Y. Zhao, D. G. Truhlar, *J. Chem. Theory Comput.,* **2010**, *6*, 2872-2887.

[22] a) B. Van der Westhuizen, P. J. Swarts, I. Strydom, D. C. Liles, I. Fernández, J. C. Swarts, D. I. Bezuidenhout, *Dalton Trans.* **2013**, *42*, 5367-5378; b) B. Van der Westhuizen, P. J. Swarts, L. M. van Jaarsveld, D. C. Liles, U. Siegert, J. C. Swarts, I. Fernández, D. I. Bezuidenhout, *Inorg. Chem.* **2013**, *52*, 6674-6684.

[23] D. I. Bezuidenhout, I. Fernández, B. Van der Westhuizen,, P. J. Swarts, J. C. Swarts, *Organometallics,* **2013**, *32*, 7334-7344.

[24] See computational details.

[25] a) D. A. Valyaev, R. Nrousses, N. Lugan, I. Fernández, M. A. Sierra, *Chem. Eur. J.* **2011**, *17(24)*, 6602-6605; b) N. Lugan, I. Fernández, R. Brousses, D. A. Valyaev, G. Lavigne, N. A. Ustynyuk, *Dalton. Trans*., **2013**, *42(4)*, 898-901.

[26] Leading references describing the electrochemical activity and behaviour of ferrocene and decamethylferrocene in a multitude of organic solvents are: a) I. Noviandri, K. N. Brown, D. S. Fleming, P. T. Gulyas, P. A. Lay, A. F. Masters and L. Phillips, *J. Phys. Chem. B*, **1999**, *103*, 6713-6722; b) N. G. Connelly and W. E. Geiger, *Chem. Rev.*, **1996**, *96*, 877-910; c) J. Ruiz and D. Astruc, C. R. *Acad. Sci., Ser. IIc: Chim.*, **1998**, *1*, 21-27; d) R. J. Aranzaes, M. C. Daniel and D. Astruc, *Can. J. Chem.*, **2006**, 84, 288-299; e) E. Fourie, J. C. Swarts, I. Chambrier, M. J. Cook, *Dalton Trans.,* **2009**, 1145-1154.

[27] N. G. Connelly, W. E. Geiger, *Adv. Organomet. Chem.*, **1984**, *23*, 49.

[28] a) H. J. Gericke, N. I. Barnard, E. Erasmus, J. C. Swarts, M. J. Cook, M. A. S. Aquino, *Inorg. Chim. Acta,* **2010**, *363*, 2222-2232; b) D. H. Evans, K. M. O'Connell, R. A. Peterson, M. J. Kelly, *J. Chem. Educ.*, **1983**, *60*, 290-293; c) P. T. Kissinger, W. R. Heineman, *J. Chem. Educ.* **1983**, *60*, 702-706. d) J. J. Van Benschoten, J. Y. Lewis, W. R. Heineman, *J. Chem. Educ.*, **1983**, *60*, 772-776; e) G. A. Mobbott, *J. Chem. Educ.*, **1983**, *60*, 697-702; f) M. J. Cook, I. Chambrier, G. F. White, E. Fourie, J. C. Swarts, *Dalton Trans.* **2009**, 1136-1144.

[29] M. Lein, *Coord. Chem. Rev*. **2009**, *253*, 625-634.
[30] a) K. L. Letchworth, D. C. Benner, *J. Quant. Spectr. Radiative Transfer*, **2007**, *107*, 173-192; b) B. H. Armstrong, *J. Quant. Spectr. Radiative Transfer*, **1967**, *7*, 61-88.
[31] A. D. McLean, G. S. Chandler, *J. Chem. Phys.*, **1980**, *72*, 5639-5648.
[32] P. Fuentealba, H. Preuss, H. Stoll, L. Von Szentpály, *Chem. Phys. Lett.* **1982**, *89,* 418-422.
[33] A. E. Reed, R. B. Weinstock, F. Weinhold. *J. Chem. Phys.* **1985**, *83*, 735-746.
[34] a) G. Gritzner and J. Kuta, *Pure Appl. Chem.*, **1984**, *56*, 461-466; b) R. R. Gagne, C. A. Koval and G. C. Lisensky, *Inorg.Chem.*, **1980**, *19*, 2854-2855.
[35] Wojdyr, M. *J. Appl. Crystallogr.* **2010**, *43*, 1126-1128.
[36] M. J. Frisch, G. W. Trucks, H. B. Schlegel, G. E. Scuseria, M. A. Robb, J. R. Cheeseman, G. Scalmani, V. Barone, B. Mennucci, G. A. Petersson, H. Nakatsuji, M. Caricato, X. Li, H. P. Hratchian, A. F. Izmaylov, J. Bloino, G. Zheng, J. L. Sonnenberg, M. Hada, M. Ehara, K. Toyota, R. Fukuda, J. Hasegawa, M. Ishida, T. Nakajima, Y. Honda, O. Kitao, H. Nakai, T. Vreven, J. A. Montgomery Jr., J. E. Peralta, F. Ogliaro, M. Bearpark, J. J. Heyd, E. Brothers, K. N. Kudin, V. N. Staroverov, R. Kobayashi, J. Normand, K. Raghavachari, A. Rendell, J. C. Burant, S. S. Iyengar, J. Tomasi, M. Cossi, N. Rega, J. M. Millam, M. Klene, J. E. Knox, J. B. Cross, V. Bakken, C. Adamo, J. Jaramillo, R. Gomperts, R. E. Stratmann, O. Yazyev, A. J. Austin, R. Cammi, C. Pomelli, J. W. Ochterski, R. L. Martin, K. Morokuma, V. G. Zakrzewski, G. A. Voth, P. Salvador, J. J. Dannenberg, S. Dapprich, A. D. Daniels, Ö. Farkas, J. B. Foresman, J. V. Ortiz, J. Cioslowski and D. J. Fox, Gaussian 09, Revision B.1, Gaussian, Inc., Wallingford, CT, 2009.
[37] a) A. D. Becke, *J. Chem. Phys.*, **1993**, *98*, 5648; b) C. Lee, W. Yang and R. G. Parr, *Phys. Rev. B: Condens. Matter*, **1988**, *37*, 785-789.
[38] F. Weigend, R. Ahlrichs, *Phys. Chem. Chem. Phys.*, **2005**, *7*, 3297-3305.
[39] J. W. McIver and A. K. Komornicki, *J. Am. Chem. Soc.*, **1972**, *94*, 2625-2633.
[40] R. F. W. Bader, *Atoms in Molecules - A Quatum Theory*, Oxford University Press, Oxford, 1990.
[41] T. A. Keith, AIMAll, 2010, http://tkgristmill.com]
[42] J. Heyd, G. Scuseria, *J. Chem. Phys.* **2004**, *121*, 1187-1192.

Entry for the Table of Contents

Layout 1:

Isolating a carbene radical cation

Daniela I. Bezuidenhout,[a] Belinda van der Westhuizen,[a] Pieter J. Swarts,[b] Teshica Chatturgoon,[c] Orde Q. Munro,[c]* Israel Fernández,[d]* and Jannie C. Swarts[b]**

Redox behaviour of cymantrenyl Fischer carbene complexes in designing organometallic multi-tags

An electrochemical and computational elucidation of the redox behaviour of Fischer carbene derivatised cymantrene complexes. The isolation of the chemically oxidised radical cation of the ferrocenylcarbene cymantrene complex was achieved, and could be characterised by FTIR and ESR spectroscopy.

Keywords: Fischer carbenes • organometallic multi-tags • electrochemistry • manganese(I) • DFT calculations • ESR spectroscopy

Schemes and Figures

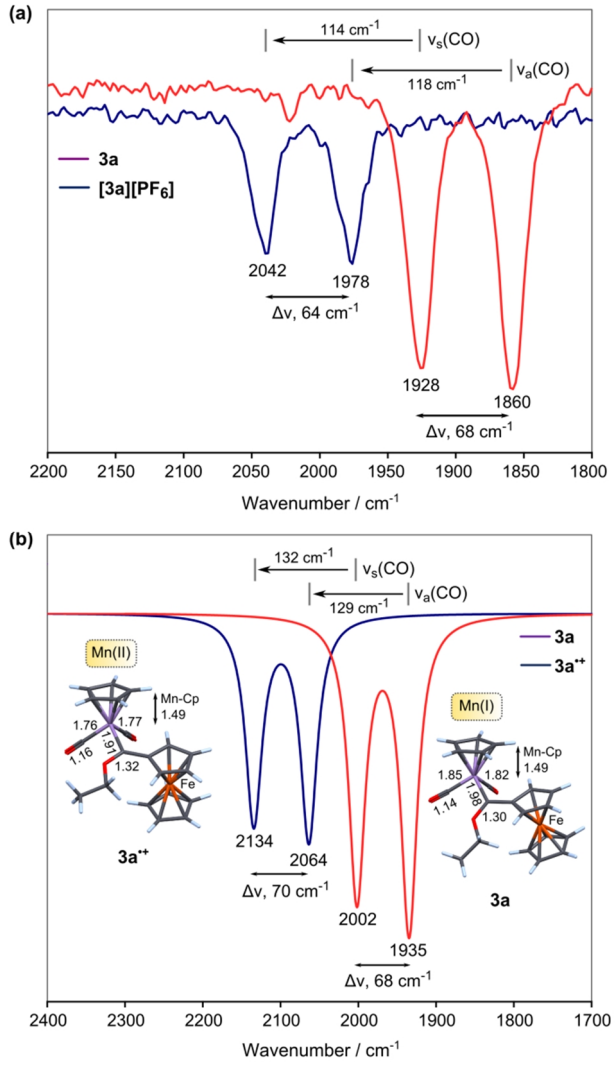

Figure 1. (a) Carbonyl region FTIR spectra of neutral **3a** and the oxidized species **[3a][PF$_6$]** in CH_2Cl_2. The antisymmetric CO stretching mode (ν_a) is at a lower wavenumber than the symmetric mode (ν_s) in each oxidation state. (b) DFT-calculated IR spectra (HWHM line width, 13 cm^{-1}) for **3a** and **3a$^{\bullet+}$** at the HSEH1PBE/6-311+g(d,p) level of theory in CH_2Cl_2 solvent (polarization continuum model, PCM). Key bond distances (Å) for the two complexes are indicated along with band shifts and splittings for comparison with the experimental spectrum.

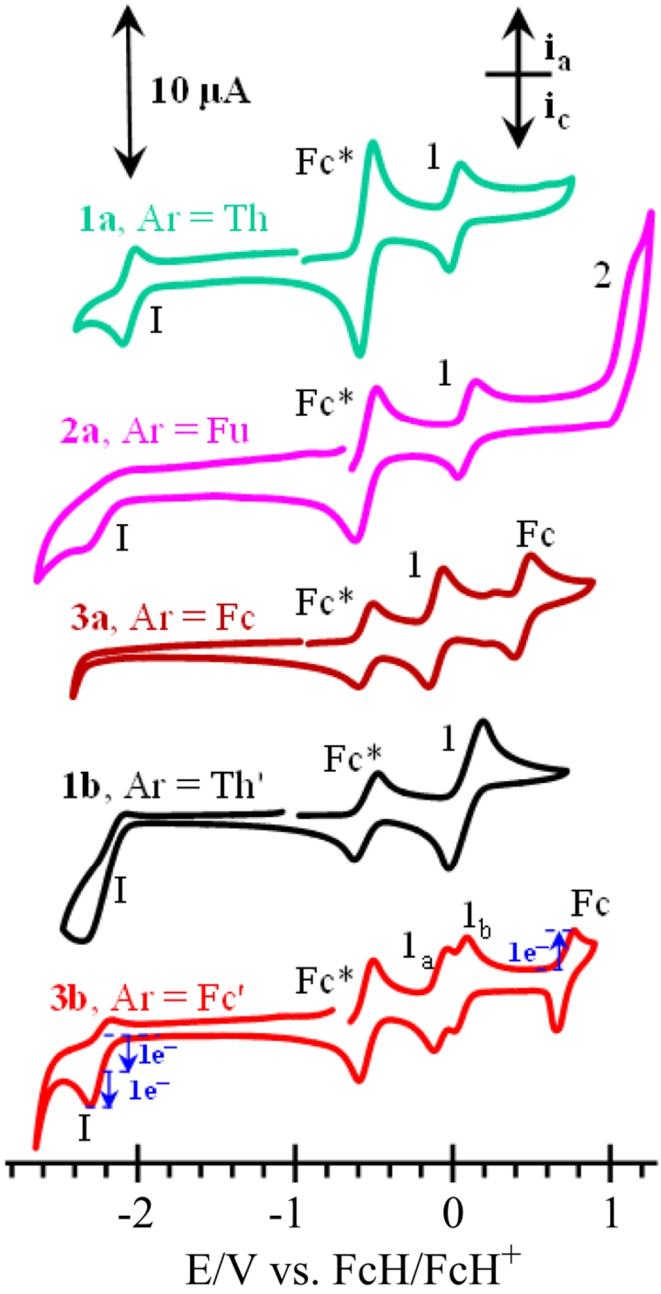

Figure 2. Cyclic voltammograms of 0.5 mmol·dm^{-3} solutions of monocarbenes **1a** (green, top), **2a** (mauve, 2nd from top) and **3a** (brown, third from the top) and biscarbene complexes [Cp(CO)$_2$Mn=C(OEt)-Ar'-(OEt)C=Mn(CO)$_2$Cp] **1b** (black 2nd from bottom) and **3b** (red, bottom) in CH_2Cl_2 containing 0.1 mol·dm^{-3} [N(^{n}Bu)$_4$][PF$_6$] as supporting electrolyte at a scan rate of 100 mV s^{-1} and 20 °C. Fc* = decamethylferrocene = internal standard. Under these conditions, each Mn centre is involved in a one-electron transfer redox process.

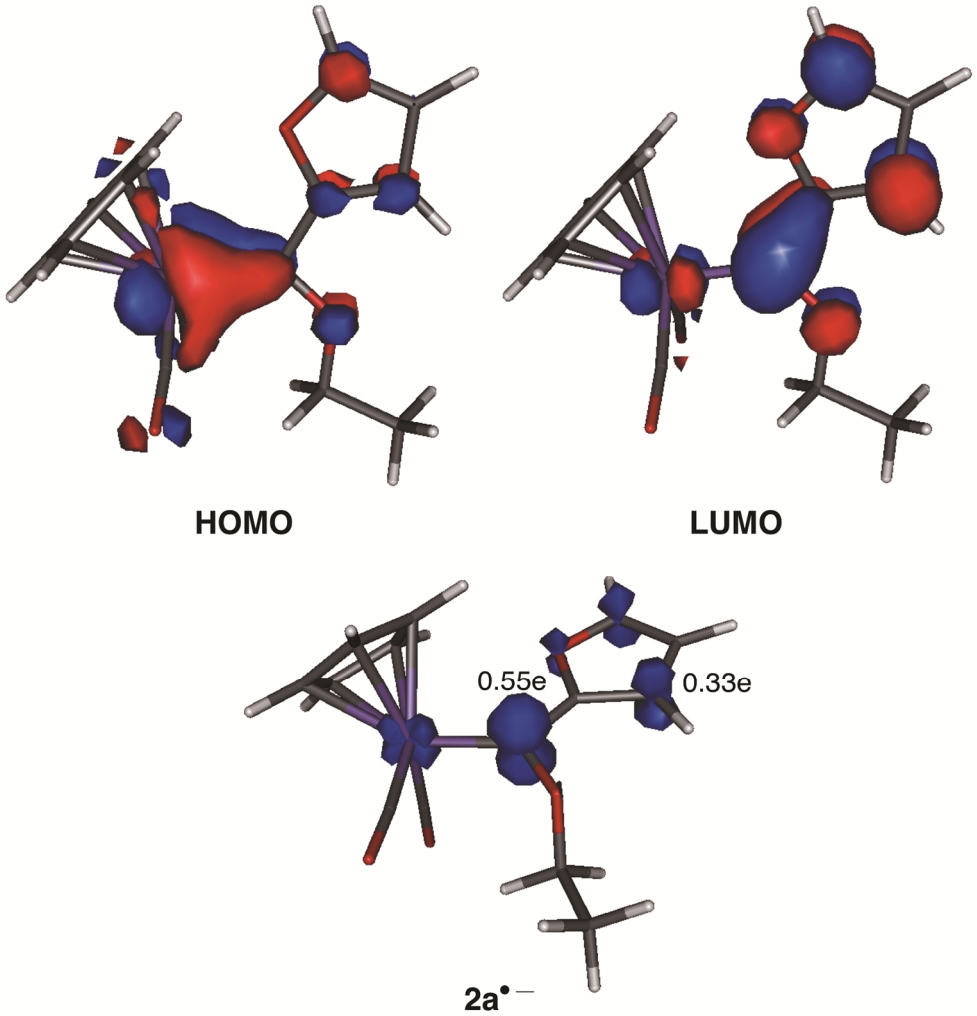

Figure 3. Computed frontier molecular orbitals of **2a** (top) and spin density of radical anion **2a**$^{\bullet-}$.

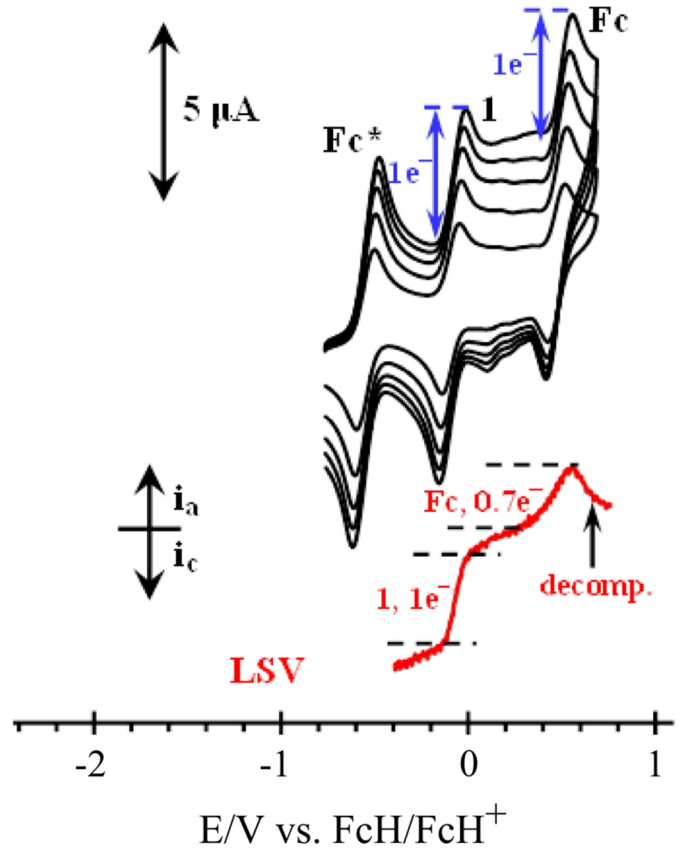

Figure 4**.** CV scans of 0.5 mmol·dm^{-3} solutions of the [(Cp)(OC)$_2$Mn=C(Fc)(OEt)], **3a**, in CH_2Cl_2 containing 0.1 mol·dm^{-3} [N(^{n}Bu)$_4$][PF$_6$] as supporting electrolyte at a scan rate of 100 (smallest currents), 200, 300, 400 and 500 mV·s^{-1} and 20 °C. The blue arrows on the CV's show the Mn centre is involved in the same number of electrons being transferred as the ferrocenyl group, that is, it involves a one-electron transfer process. The LSV shows that the doubly oxidised **3a** is unstable on LSV time scale (1 mV·s^{-1}; currents were enlarged three fold for clarity): the compound begins to decompose notably after 0.7 electrons have flown during Fc oxidation. Fc* = decamethylferrocene.

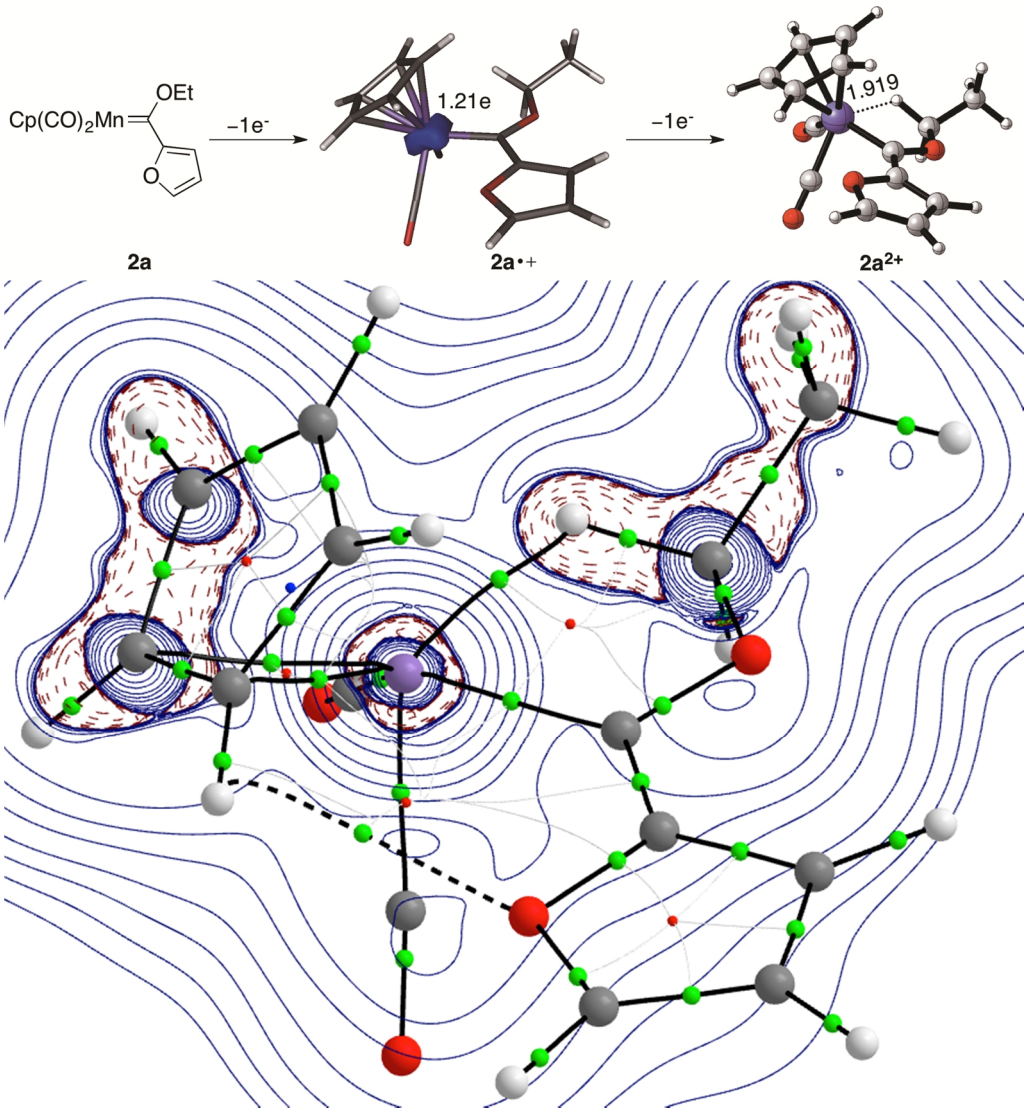

Figure 5. (a) Oxidation process of complex **2a**. (b) Contour line diagrams $\nabla^2\rho(r)$ for complex **2a**$^{2+}$ in the Mn−H−C plane. The solid lines connecting the atomic nuclei are the bond paths while the small red spheres indicate the corresponding bond critical points.

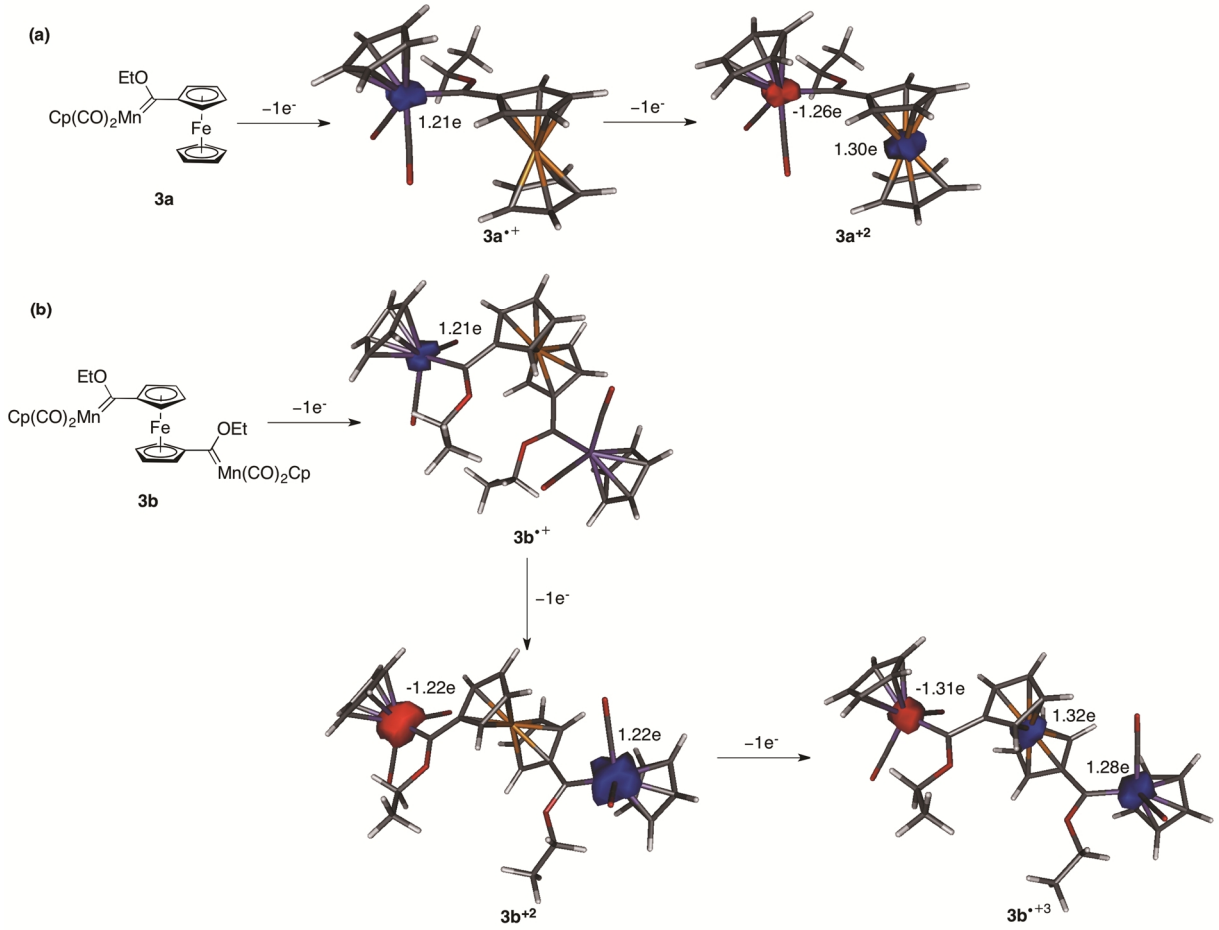

Figure 6. Oxidation processes of complexes **3a** (a) and **3b** (b). Spin densities were computed at the B3LYP/def2-SVP level.

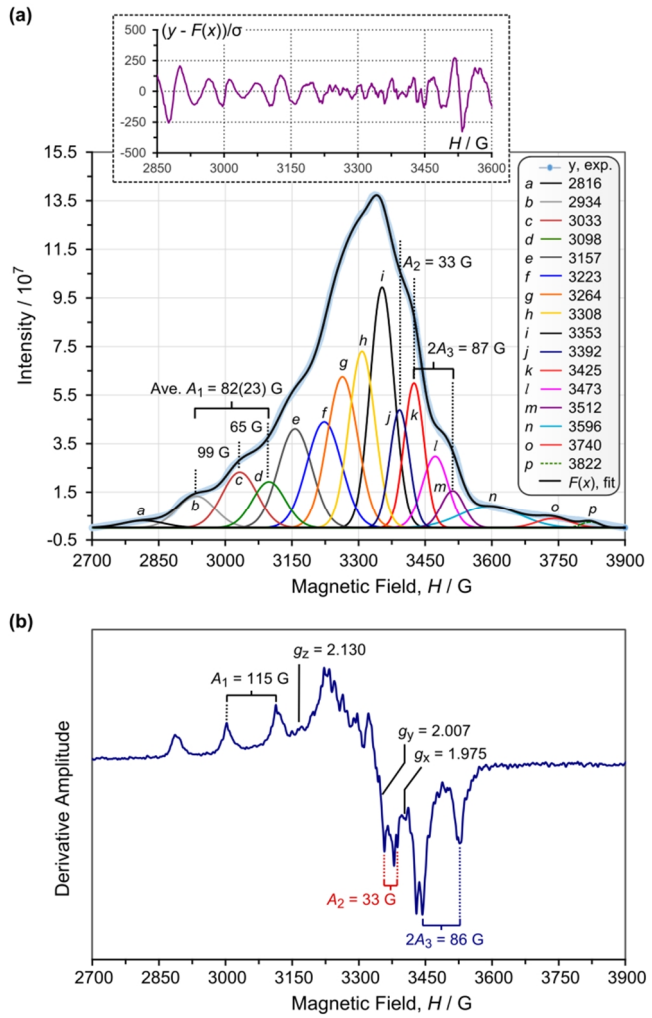

Figure 7. (a) ESR absorption spectrum of **[3a][PF_6]** recorded in CH_2Cl_2 at 77 K shortly after oxidation of **3a** with $AgPF_6$. The spectral envelope is deconvoluted into a series of Voigt functions; the sum of these, $F(x)$, fits the experimental spectrum with a correlation coefficient of 0.9999. The raw spectral data are shown without background subtraction; the first (2816 G) and last three (≥ 3596 G) bands simply match the background and may be ignored. The upper inset shows the weighted fit residuals for the spectral region containing useful spectroscopic information; the right inset lists the H_{max} values for the Voigt components. (b) Derivative mode ESR spectrum (12 scans) of **[3a][PF_6]** with assigned *g*-tensor components. Data acquisition: frequency, 9.421260 GHz; attenuation, 20.0 dB; power, 2.00 mW; modulation amplitude, 2.00 G (modulation frequency 100.00 kHz); time constant, 81.92 ms; conversion time, 38.00 ms; sweep width, 1200 G (centre field = 3300 G); data resolution, 2400 points.

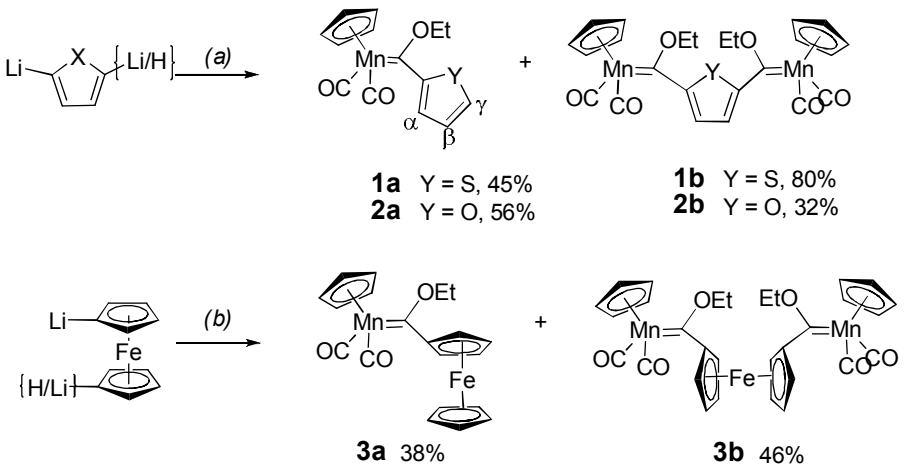

Scheme 1. Reagents and conditions: (a) (i) 2 eq $CpMn(CO)_3$, thf, –60 °C; (ii) excess Et_3OBF_4, CH_2Cl_2, –40 °C. (b) (i) 2 eq $CpMn(CO)_3$, thf, –50 °C; (iii) excess Et_3OBF_4, CH_2Cl_2, –40 °C.

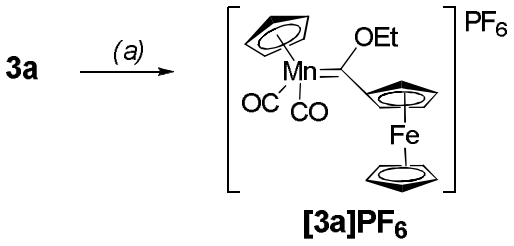

Scheme 2: Reagents and conditions: (a) 1 eq $AgPF_6$, CH_2Cl_2, –35 °C.

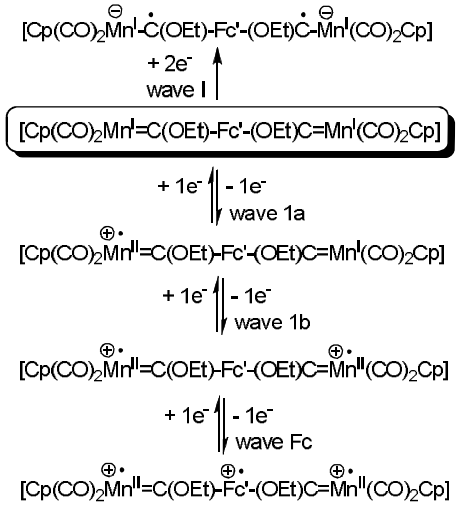

Scheme 3. Electrochemical reactions associated with **3b**.

Supporting Information

Figure S1
Figure S2
Table S1
Table S2
Table S3
Table S4
Table S5
Table S6
Table S7
Table S8
Table S9
Table S10
References

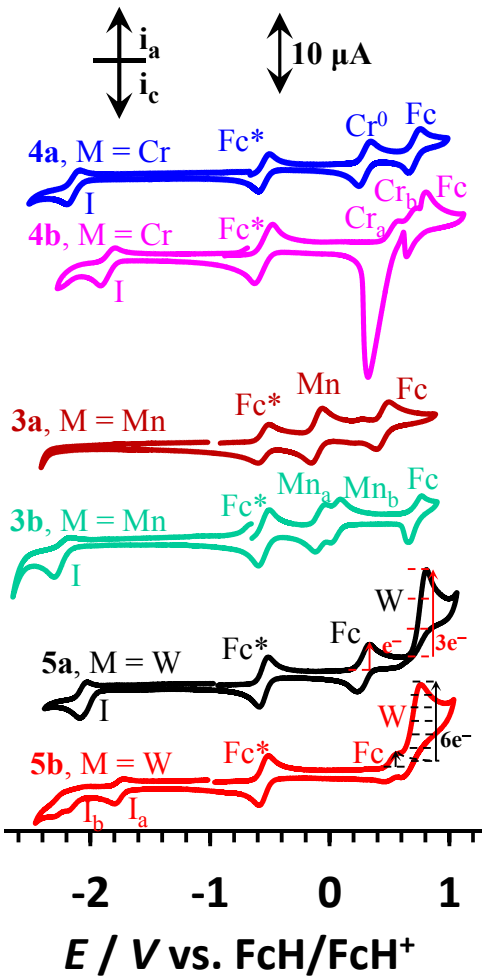

Figure S1. CV's of 0.5 mmol·dm^{-3} solutions of monocarbene ferrocenyl complexes **3a** [$Cp(CO)_2Mn{=}C(OEt)Fc$], **2a** [$(CO)_5Cr{=}C(OEt)Fc$][1], and **5a** [$(CO)_5W{=}C(OEt)Fc$][2], and biscarbene complexes **3b** [$Cp(CO)_2Mn{=}C(OEt)$-Fc'-$(OEt)C{=}Mn(CO)_2Cp$], **4b** [$(CO)_5Cr{=}C(OEt)$-Fc'-$(OEt)C{=}Cr(CO)_5$][1] and **5b** [$(CO)_5W{=}C(OEt)$-Fc'-$(OEt)C{=}W(CO)_5$][2] in CH_2Cl_2 containing 0.1 mol·dm^{-3} [$N(^nBu)_4$][PF_6] as supporting electrolyte at a scan rate of 100 mV s^{-1} and 20 °C. Fc* = decamethylferrocene = internal standard.

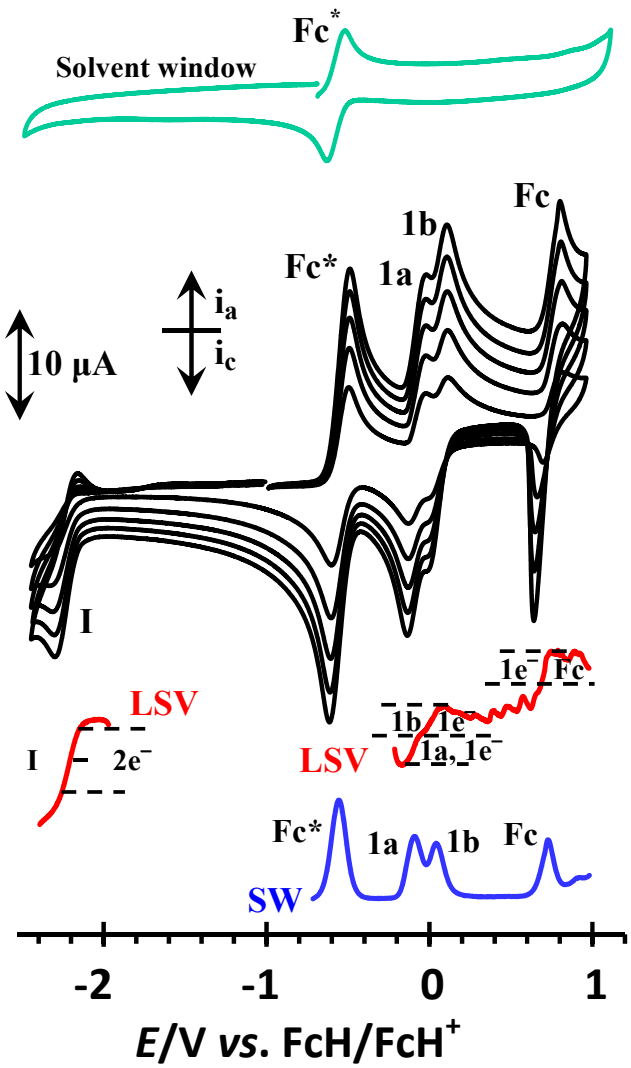

Figure S2. CV's (black traces) of 0.5 mmol·dm^{-3} solutions of biscarbene complexes **3b** [$Cp(CO)_2Mn=C(OEt)$-Fc'-$(OEt)C=Mn(CO)_2Cp$], at scan rates of 100 (smallest currents), 200, 300, 400 and 500 mV s^{-1} in CH_2Cl_2 containing 0.2 mol·dm^{-3} [N(^{n}Bu)$_4$][PF_6] as supporting electrolyte. LSV's (red traces) at 2 mV s^{-1} and an SW at 60 Hz is also shown. Fc* = decamethylferrocene = internal standard, temperature 20 ^{o}C.

Table S1. Cartesian coordinates (in Å) and total energies (in a. u., zero-point vibrational energy included) of all the stationary points discussed in the text. All calculations have been performed at the B3LYP/def2-SVP level.

2a: E= -1992.210154

C	1.538414000	0.921776000	1.321873000
C	1.562945000	0.938911000	-1.296965000
C	-0.778128000	0.404065000	-0.004732000
C	2.033960000	-1.771263000	1.139198000
H	2.353596000	-1.661010000	2.174781000
C	2.822965000	-1.477328000	-0.010008000
H	3.844098000	-1.100289000	-0.012450000
C	2.025461000	-1.763684000	-1.155885000
H	2.337658000	-1.646839000	-2.193001000
C	0.759970000	-2.240485000	-0.718094000
H	-0.059839000	-2.552144000	-1.358513000
C	0.764978000	-2.245347000	0.707705000
H	-0.050118000	-2.561421000	1.351946000
C	-2.007262000	-0.408103000	-0.004049000
O	-1.963025000	-1.774506000	0.005126000
C	-3.227974000	-2.238690000	0.003283000
H	-3.341853000	-3.320215000	0.010110000
C	-4.122716000	-1.201495000	-0.007112000
H	-5.207848000	-1.280653000	-0.010899000
C	-3.335948000	-0.016794000	-0.011715000
H	-3.683730000	1.011597000	-0.019785000
O	1.925131000	1.549124000	2.214535000
O	1.975710000	1.578176000	-2.169354000
O	-1.257742000	1.660124000	-0.007118000
Mn	1.050725000	-0.178436000	0.000512000
C	-0.474959000	2.853777000	-0.012155000
H	0.180485000	2.870792000	0.870668000
H	0.159412000	2.875338000	-0.910235000
C	-1.432410000	4.030685000	0.002230000
H	-2.065621000	4.013898000	0.902729000
H	-2.086811000	4.018671000	-0.883079000
H	-0.863927000	4.973676000	-0.002029000

3a: E= -3412.653072

C	2.654815000	-0.660137000	-1.850294000
C	3.739808000	-0.066485000	-1.144384000
C	4.150889000	-0.988469000	-0.128880000
C	3.317115000	-2.131928000	-0.211391000
C	2.390075000	-1.936314000	-1.285636000
Mn	2.085254000	-0.397063000	0.263104000
C	1.128189000	-1.328292000	1.444270000
O	0.545490000	-1.966623000	2.217898000

C	0.545637000	0.576225000	-0.367799000
O	0.368205000	1.888600000	-0.488951000
C	1.338918000	2.872900000	-0.104837000
C	0.912629000	4.199908000	-0.701325000
C	-0.625515000	-0.066273000	-0.996416000
C	-1.607662000	0.610181000	-1.819850000
C	-2.570235000	-0.343031000	-2.245341000
C	-2.221609000	-1.610259000	-1.682277000
C	-1.036106000	-1.447407000	-0.915243000
Fe	-2.520989000	-0.214327000	-0.164854000
C	-3.828468000	1.161345000	0.680803000
C	-2.680362000	0.998737000	1.511962000
C	-2.605088000	-0.374240000	1.904872000
C	-3.710039000	-1.058295000	1.315043000
C	-4.465134000	-0.112566000	0.555711000
C	2.623022000	0.740064000	1.522234000
O	3.067754000	1.407190000	2.361256000
H	-1.588220000	1.667328000	-2.071583000
H	-0.544498000	-2.225658000	-0.339458000
H	-2.780922000	-2.537536000	-1.799007000
H	-3.437686000	-0.139442000	-2.872023000
H	2.329883000	2.559956000	-0.463716000
H	1.378332000	2.923093000	0.992991000
H	-1.826285000	-0.827125000	2.515960000
H	-3.924763000	-2.122125000	1.407047000
H	-5.360635000	-0.326722000	-0.026112000
H	-4.150807000	2.087784000	0.207576000
H	-1.966251000	1.777702000	1.775141000
H	1.629409000	4.984679000	-0.413589000
H	0.879451000	4.148633000	-1.800708000
H	-0.084167000	4.495592000	-0.339223000
H	4.963239000	-0.837566000	0.580404000
H	3.382800000	-3.015196000	0.422342000
H	4.200986000	0.895207000	-1.362535000
H	1.636526000	-2.643186000	-1.625491000
H	2.121117000	-0.213660000	-2.688351000

3b: E= -5175.074320

Mn	-3.718216000	-0.456792000	-0.264747000
C	-2.061658000	-0.207440000	0.708130000
O	-1.315675000	-1.131156000	1.300901000
C	-3.286498000	0.681013000	-1.561722000
O	-3.086271000	1.419659000	-2.434413000
C	-3.154808000	-1.841688000	-1.229481000
O	-2.851159000	-2.743981000	-1.895534000
C	-4.779136000	-0.333816000	1.665264000
H	-4.287374000	-0.275519000	2.635623000
C	-5.172099000	-1.528157000	1.002066000
H	-5.063161000	-2.542468000	1.382102000
C	-5.789123000	-1.155999000	-0.235491000
H	-6.206306000	-1.839295000	-0.973466000
C	-5.776549000	0.259013000	-0.321847000

H	-6.183664000	0.850811000	-1.140582000
C	-5.151932000	0.777221000	0.857325000
H	-5.016364000	1.826945000	1.109067000
Mn	3.718261000	-0.456281000	0.264836000
C	2.061715000	-0.207259000	-0.708117000
O	1.316099000	-1.131189000	-1.301035000
C	3.154798000	-1.840793000	1.230103000
O	2.851110000	-2.742807000	1.896519000
C	3.286468000	0.681926000	1.561399000
O	3.086150000	1.420836000	2.433848000
C	4.779327000	-0.337467000	-1.665446000
H	4.287585000	-0.282192000	-2.635993000
C	5.173373000	-1.529627000	-0.999105000
H	5.065285000	-2.545051000	-1.376418000
C	5.789959000	-1.153697000	0.237541000
H	6.207675000	-1.834648000	0.977372000
C	5.776011000	0.261535000	0.320147000
H	6.182378000	0.855854000	1.137432000
C	5.150972000	0.776090000	-0.860318000
H	5.014362000	1.825025000	-1.114773000
Fe	-0.000213000	2.113774000	-0.000113000
C	-1.466582000	1.094568000	1.064746000
C	-1.924944000	2.412590000	0.694754000
H	-2.780787000	2.637317000	0.065608000
C	-1.054496000	3.370600000	1.281297000
H	-1.132658000	4.451084000	1.168042000
C	-0.041065000	2.672637000	2.011403000
H	0.797434000	3.117300000	2.544537000
C	-0.284271000	1.283089000	1.879390000
H	0.316618000	0.484224000	2.303612000
C	1.466280000	1.094553000	-1.064762000
C	0.283936000	1.282737000	-1.879435000
H	-0.316829000	0.483692000	-2.303494000
C	0.040506000	2.672218000	-2.011731000
H	-0.798070000	3.116618000	-2.544963000
C	1.053854000	3.370481000	-1.281796000
H	1.131855000	4.450996000	-1.168704000
C	1.924455000	2.412728000	-0.695055000
H	2.780288000	2.637811000	-0.066015000
C	-1.600364000	-2.539776000	1.284245000
H	-1.278622000	-2.947029000	0.314053000
H	-2.685344000	-2.684928000	1.365278000
C	-0.850765000	-3.183401000	2.434334000
H	-1.046235000	-4.267349000	2.440106000
H	-1.181936000	-2.770134000	3.399694000
H	0.235660000	-3.031614000	2.347181000
C	1.601156000	-2.539729000	-1.284167000
H	1.279723000	-2.946930000	-0.313849000
H	2.686157000	-2.684601000	-1.365387000
C	0.851497000	-3.183757000	-2.433997000
H	1.047014000	-4.267695000	-2.439433000
H	1.182533000	-2.770782000	-3.399527000
H	-0.234927000	-3.031997000	-2.346758000

2a$^{\cdot-}$: E= -1992.240027

C	1.710577000	1.452333000	0.448670000
C	1.020875000	0.345472000	-1.769439000
C	-0.778261000	0.335147000	0.218043000
C	1.933234000	-1.264885000	1.675098000
H	1.977875000	-0.854053000	2.682721000
C	2.946383000	-1.145707000	0.666525000
H	3.906050000	-0.642036000	0.778832000
C	2.481098000	-1.810138000	-0.498496000
H	3.023356000	-1.902145000	-1.439418000
C	1.180687000	-2.341870000	-0.222974000
H	0.539603000	-2.886041000	-0.911578000
C	0.852981000	-1.991855000	1.115334000
H	-0.088358000	-2.217286000	1.610174000
C	-1.931183000	-0.475939000	0.135817000
O	-1.838417000	-1.804613000	-0.264173000
C	-3.091031000	-2.343545000	-0.251157000
H	-3.168287000	-3.386799000	-0.548715000
C	-4.012051000	-1.407308000	0.151009000
H	-5.085655000	-1.569556000	0.252878000
C	-3.293357000	-0.210616000	0.404609000
H	-3.677223000	0.742967000	0.755241000
O	2.153922000	2.468941000	0.819926000
O	0.958667000	0.634408000	-2.899920000
O	-1.183840000	1.623624000	0.637535000
Mn	1.154988000	-0.135179000	-0.077082000
C	-1.143366000	2.646444000	-0.327799000
H	-0.177691000	2.640865000	-0.865432000
H	-1.933747000	2.488254000	-1.093360000
C	-1.337042000	3.982925000	0.371685000
H	-0.515274000	4.155534000	1.084340000
H	-2.286971000	3.998456000	0.931441000
H	-1.348277000	4.809679000	-0.358559000

2a$^{\cdot+}$: E= -1991.991076

C	0.341886000	-1.622427000	1.353039000
C	1.748514000	0.492970000	1.485810000
C	-0.754890000	0.675636000	0.054328000
C	1.899168000	-2.075599000	-1.022369000
H	1.942800000	-3.104518000	-0.665512000
C	2.859920000	-1.066110000	-0.761234000
H	3.778502000	-1.189641000	-0.188863000
C	2.420371000	0.134809000	-1.404227000
H	2.965908000	1.077329000	-1.430678000
C	1.184062000	-0.146100000	-2.058339000
H	0.606003000	0.547331000	-2.667957000
C	0.858535000	-1.513087000	-1.813563000
H	-0.026538000	-2.037834000	-2.169793000
C	-2.038387000	0.047046000	-0.037574000

O	-2.103376000	-1.324791000	-0.070172000
C	-3.396835000	-1.667251000	-0.147230000
H	-3.614285000	-2.733383000	-0.177023000
C	-4.204408000	-0.550950000	-0.170446000
H	-5.290835000	-0.540282000	-0.227696000
C	-3.331198000	0.557371000	-0.100446000
H	-3.593635000	1.612957000	-0.091515000
O	0.008288000	-2.383666000	2.130520000
O	2.271020000	1.018923000	2.353229000
O	-0.893760000	1.974587000	0.045110000
Mn	0.932307000	-0.391731000	0.075432000
C	0.210446000	2.913185000	0.139090000
H	0.501016000	2.968552000	1.199532000
H	1.055066000	2.513538000	-0.440643000
C	-0.260058000	4.253393000	-0.379070000
H	-1.115286000	4.623934000	0.205022000
H	-0.553681000	4.192521000	-1.437661000
H	0.557152000	4.985056000	-0.289122000

2a^{2+}: E= -1991.538744

O	-1.070654000	1.666773000	-0.433211000
O	0.194664000	-0.434235000	-2.911922000
C	-0.935678000	0.400307000	-0.149962000
C	-2.092925000	-0.354397000	0.026567000
C	-2.311032000	-1.711204000	0.346910000
H	-1.544790000	-2.463103000	0.526576000
C	-3.693322000	-1.899586000	0.388123000
H	-4.240066000	-2.816317000	0.603277000
C	-4.250958000	-0.655263000	0.092541000
H	-5.287823000	-0.323855000	0.011476000
C	0.118191000	2.456119000	-0.685315000
H	0.199631000	2.584524000	-1.775387000
H	1.048147000	1.878784000	-0.348056000
C	0.058017000	3.770935000	0.050591000
H	0.945335000	4.374070000	-0.194462000
H	0.003259000	3.636909000	1.140593000
H	-0.831958000	4.327538000	-0.283187000
C	0.549261000	-0.278937000	-1.847411000
C	0.531225000	0.511660000	1.689312000
O	0.168726000	0.824420000	2.715972000
O	-3.318436000	0.259115000	-0.121782000
C	2.729976000	-0.662479000	1.272747000
C	1.816707000	-1.781217000	1.070135000
C	3.289140000	-0.304113000	0.024108000
H	3.006340000	-0.232795000	2.237606000
C	1.819888000	-2.088854000	-0.294058000
H	1.274934000	-2.309460000	1.855843000
C	2.736239000	-1.164932000	-0.952356000
H	4.011736000	0.493957000	-0.154162000
H	1.280588000	-2.903331000	-0.779622000
H	3.018298000	-1.190582000	-2.006775000
Mn	1.085344000	-0.040527000	-0.040710000

3a$^{\cdot+}$: E= -3412.436669

C	3.067529000	-0.010308000	-1.704505000
C	4.009396000	-0.019868000	-0.635659000
C	4.039689000	-1.341197000	-0.085107000
C	3.123250000	-2.137648000	-0.823027000
C	2.517032000	-1.320929000	-1.815497000
Mn	2.044224000	-0.461368000	0.163702000
C	1.049902000	-1.682640000	1.131812000
O	0.472977000	-2.450517000	1.749443000
C	0.500544000	0.710466000	-0.361701000
O	0.480720000	2.018567000	-0.314844000
C	1.506484000	2.843753000	0.288800000
C	1.306542000	4.267183000	-0.182492000
C	-0.660623000	0.205971000	-1.052043000
C	-1.690318000	1.038554000	-1.659978000
C	-2.653557000	0.185758000	-2.247151000
C	-2.280363000	-1.170572000	-1.989342000
C	-1.073748000	-1.174401000	-1.247080000
Fe	-2.511042000	-0.138413000	-0.180557000
C	-3.723459000	1.061372000	1.018226000
C	-2.645004000	0.539661000	1.788555000
C	-2.717439000	-0.888832000	1.751125000
C	-3.848153000	-1.246226000	0.958695000
C	-4.466848000	-0.044092000	0.500937000
C	2.420255000	0.289885000	1.815605000
O	2.673139000	0.721319000	2.841897000
H	-1.684255000	2.125194000	-1.684247000
H	-0.551117000	-2.066906000	-0.913057000
H	-2.842231000	-2.053887000	-2.288985000
H	-3.547074000	0.507821000	-2.780046000
H	2.491368000	2.448392000	-0.000516000
H	1.399024000	2.763781000	1.381461000
H	-2.040523000	-1.582694000	2.245909000
H	-4.172099000	-2.259682000	0.725985000
H	-5.345767000	0.019008000	-0.139082000
H	-3.935988000	2.114621000	0.841515000
H	-1.890628000	1.129754000	2.307573000
H	2.063899000	4.916117000	0.282787000
H	1.410352000	4.343899000	-1.275138000
H	0.312757000	4.641662000	0.104264000
H	4.672271000	-1.683747000	0.732678000
H	2.914397000	-3.193407000	-0.651260000
H	4.631786000	0.815750000	-0.317404000
H	1.763859000	-1.638701000	-2.535173000
H	2.830099000	0.835647000	-2.348315000

3a^{2+}: E= -3412.091750

C	2.819633000	-0.433088000	-1.871304000
C	3.859614000	0.087744000	-1.046366000
C	4.261400000	-0.940927000	-0.142293000

C	3.471483000	-2.088382000	-0.394585000
C	2.568592000	-1.778459000	-1.459799000
Mn	2.102488000	-0.430670000	0.164437000
C	1.080943000	-1.601711000	1.159012000
O	0.431498000	-2.314160000	1.772200000
C	0.549699000	0.688950000	-0.331351000
O	0.466057000	1.979978000	-0.251213000
C	1.519210000	2.865465000	0.263971000
C	1.294695000	4.251457000	-0.291285000
C	-0.672008000	0.176909000	-1.003583000
C	-1.642464000	1.013461000	-1.683517000
C	-2.576204000	0.170642000	-2.336377000
C	-2.228864000	-1.182956000	-2.059806000
C	-1.068978000	-1.190772000	-1.242827000
Fe	-2.592306000	-0.140482000	-0.186306000
C	-3.959002000	1.017923000	0.891387000
C	-2.871747000	0.674312000	1.753339000
C	-2.836932000	-0.747193000	1.877759000
C	-3.892893000	-1.285817000	1.094097000
C	-4.588810000	-0.200324000	0.480165000
C	2.597713000	0.345084000	1.814381000
O	2.913633000	0.779977000	2.814954000
H	-1.630013000	2.101640000	-1.710054000
H	-0.580403000	-2.088278000	-0.870441000
H	-2.778141000	-2.064064000	-2.393438000
H	-3.433456000	0.501987000	-2.923871000
H	2.486759000	2.439838000	-0.036634000
H	1.434724000	2.842177000	1.360982000
H	-2.110745000	-1.326459000	2.448620000
H	-4.116937000	-2.345298000	0.964543000
H	-5.452117000	-0.286206000	-0.180576000
H	-4.265224000	2.025702000	0.610522000
H	-2.191020000	1.376233000	2.234741000
H	2.066425000	4.924793000	0.112346000
H	1.371854000	4.265053000	-1.388482000
H	0.313520000	4.648774000	0.007524000
H	5.044817000	-0.858743000	0.611886000
H	3.549659000	-3.043459000	0.125067000
H	4.312604000	1.076008000	-1.124779000
H	1.871221000	-2.474628000	-1.924294000
H	2.344253000	0.083945000	-2.704275000

3b$^{\cdot+}$: E= -5174.857950

Mn	-3.696867000	-0.436984000	-0.307512000
C	-2.119745000	-0.203186000	0.760709000
O	-1.437947000	-1.127895000	1.434649000
C	-3.211235000	0.731307000	-1.556399000
O	-2.968705000	1.489093000	-2.401418000
C	-3.040638000	-1.806916000	-1.242371000
O	-2.645141000	-2.687812000	-1.886836000
C	-4.915566000	-0.389619000	1.527563000
H	-4.516659000	-0.369950000	2.541215000

C	-5.251970000	-1.554434000	0.787861000
H	-5.183164000	-2.583686000	1.135759000
C	-5.764606000	-1.133184000	-0.481212000
H	-6.124907000	-1.785689000	-1.274803000
C	-5.747114000	0.283557000	-0.510415000
H	-6.090618000	0.907144000	-1.334648000
C	-5.215660000	0.754323000	0.731793000
H	-5.112449000	1.793747000	1.036856000
Mn	3.740615000	-0.449013000	0.179992000
C	1.988900000	-0.199456000	-0.771323000
O	1.268129000	-1.136814000	-1.324988000
C	3.175551000	-1.803026000	1.300815000
O	2.836394000	-2.628630000	2.014636000
C	3.376867000	0.660322000	1.618359000
O	3.190117000	1.322415000	2.529607000
C	4.793648000	-0.727584000	-1.711167000
H	4.307759000	-0.971030000	-2.655197000
C	5.282195000	-1.657557000	-0.748556000
H	5.250474000	-2.743540000	-0.829018000
C	5.877491000	-0.915753000	0.320861000
H	6.364022000	-1.332972000	1.201384000
C	5.756613000	0.465516000	0.006514000
H	6.114743000	1.292361000	0.619544000
C	5.084290000	0.585427000	-1.240075000
H	4.834433000	1.516261000	-1.747579000
Fe	0.026988000	2.093787000	0.064088000
C	-1.478686000	1.091569000	1.105090000
C	-1.907118000	2.415017000	0.734995000
H	-2.749251000	2.656370000	0.093255000
C	-1.029863000	3.359451000	1.333782000
H	-1.091391000	4.441251000	1.223763000
C	-0.044342000	2.644891000	2.083581000
H	0.777464000	3.085106000	2.646520000
C	-0.313070000	1.260335000	1.945632000
H	0.246801000	0.446186000	2.397906000
C	1.451620000	1.103906000	-1.077684000
C	0.245703000	1.340122000	-1.854889000
H	-0.375966000	0.569830000	-2.301289000
C	0.037474000	2.734147000	-1.936963000
H	-0.801050000	3.212103000	-2.440119000
C	1.075154000	3.391513000	-1.203224000
H	1.173211000	4.466717000	-1.061059000
C	1.937078000	2.408094000	-0.657818000
H	2.820930000	2.616186000	-0.060140000
C	-1.794172000	-2.522989000	1.471819000
H	-1.512557000	-2.981995000	0.512117000
H	-2.882848000	-2.610170000	1.573842000
C	-1.064211000	-3.162664000	2.635742000
H	-1.314439000	-4.233576000	2.685791000
H	-1.356670000	-2.698475000	3.589846000
H	0.028248000	-3.072933000	2.529677000
C	1.534016000	-2.559659000	-1.244517000
H	1.114296000	-2.913375000	-0.290121000

H	2.622808000	-2.712400000	-1.230981000
C	0.877158000	-3.237153000	-2.427177000
H	1.061755000	-4.321000000	-2.370701000
H	1.292633000	-2.867259000	-3.376703000
H	-0.210335000	-3.074477000	-2.426564000

$3b^{2+}$: E= -5174.561800

Mn	-4.552710000	-0.054431000	0.176723000
C	-2.741074000	0.500120000	-0.446602000
O	-2.335884000	1.722018000	-0.647425000
C	-3.938335000	-1.241622000	1.452249000
O	-3.572693000	-1.972466000	2.250271000
C	-4.779719000	1.134522000	1.602135000
O	-4.939032000	1.839392000	2.482507000
C	-5.258571000	-0.068219000	-1.861375000
H	-4.684349000	0.282309000	-2.718124000
C	-6.160845000	0.708858000	-1.076884000
H	-6.403389000	1.761157000	-1.222381000
C	-6.759001000	-0.155959000	-0.107875000
H	-7.501602000	0.131008000	0.636515000
C	-6.228990000	-1.455519000	-0.292004000
H	-6.489566000	-2.338256000	0.291989000
C	-5.292162000	-1.407486000	-1.366106000
H	-4.733040000	-2.252909000	-1.764651000
Mn	4.552349000	-0.054703000	-0.177234000
C	2.741188000	0.500245000	0.446919000
O	2.336536000	1.722300000	0.647864000
C	4.778774000	1.134236000	-1.602786000
O	4.937391000	1.839248000	-2.483163000
C	3.937111000	-1.241925000	-1.452327000
O	3.570846000	-1.972916000	-2.249930000
C	5.258714000	-0.069336000	1.860657000
H	4.684563000	0.280565000	2.717708000
C	6.160623000	0.708444000	1.076422000
H	6.402910000	1.760726000	1.222475000
C	6.758843000	-0.155654000	0.106838000
H	7.501179000	0.131958000	-0.637568000
C	6.229197000	-1.455459000	0.290277000
H	6.489918000	-2.337790000	-0.294264000
C	5.292540000	-1.408302000	1.364599000
H	4.733759000	-2.254124000	1.762780000
Fe	0.000101000	-1.150190000	0.000492000
C	-1.737671000	-0.444736000	-0.932709000
C	-1.748355000	-1.888770000	-0.846754000
H	-2.478339000	-2.505562000	-0.329403000
C	-0.634985000	-2.385639000	-1.571071000
H	-0.370646000	-3.436171000	-1.684490000
C	0.093730000	-1.276317000	-2.095030000
H	1.000007000	-1.342957000	-2.694173000
C	-0.558218000	-0.082770000	-1.691569000
H	-0.259838000	0.933908000	-1.935885000
C	1.737850000	-0.444478000	0.933451000

C	0.558360000	-0.082313000	1.692227000
H	0.259969000	0.934430000	1.936237000
C	-0.093577000	-1.275776000	2.095994000
H	-0.999850000	-1.342289000	2.695138000
C	0.635197000	-2.385209000	1.572351000
H	0.370890000	-3.435723000	1.686014000
C	1.748602000	-1.888482000	0.847940000
H	2.478593000	-2.505402000	0.330747000
C	-3.120432000	2.916477000	-0.363253000
H	-3.037917000	3.108266000	0.717469000
H	-4.170127000	2.704889000	-0.609843000
C	-2.561441000	4.060161000	-1.178347000
H	-3.132166000	4.974935000	-0.957521000
H	-2.639602000	3.859944000	-2.257254000
H	-1.507234000	4.249196000	-0.926925000
C	3.121464000	2.916377000	0.363151000
H	3.037784000	3.108461000	-0.717444000
H	4.171330000	2.704097000	0.608409000
C	2.564116000	4.060171000	1.179216000
H	3.135056000	4.974690000	0.957882000
H	2.643512000	3.859668000	2.257981000
H	1.509695000	4.249840000	0.929168000

3b$^{\cdot+3}$: E= -5174.126832

Mn	4.645584000	-0.039273000	-0.173223000
C	2.848910000	0.502197000	0.431353000
O	2.417281000	1.710360000	0.621298000
C	3.980379000	-1.173468000	-1.468189000
O	3.536793000	-1.866465000	-2.261236000
C	4.966928000	1.199363000	-1.577157000
O	5.180972000	1.918644000	-2.427681000
C	5.342101000	-0.313700000	1.852063000
H	4.760295000	-0.116945000	2.752187000
C	6.224620000	0.604361000	1.210134000
H	6.427394000	1.630090000	1.519277000
C	6.867030000	-0.080728000	0.134770000
H	7.612569000	0.343402000	-0.539348000
C	6.378565000	-1.409213000	0.098948000
H	6.690811000	-2.184349000	-0.601619000
C	5.424268000	-1.558935000	1.153952000
H	4.920776000	-2.485995000	1.426503000
Mn	-4.645739000	-0.048057000	0.169162000
C	-2.853445000	0.513658000	-0.432744000
O	-2.431139000	1.727684000	-0.606227000
C	-4.958560000	1.164978000	1.596330000
O	-5.166717000	1.869351000	2.460754000
C	-3.964933000	-1.202901000	1.437837000
O	-3.509637000	-1.907666000	2.213631000
C	-5.356042000	-0.299336000	-1.855087000
H	-4.779015000	-0.094223000	-2.756420000
C	-6.232835000	0.613573000	-1.198218000
H	-6.435588000	1.642757000	-1.495577000

C	-6.869555000	-0.081061000	-0.125744000
H	-7.609820000	0.337767000	0.557435000
C	-6.383283000	-1.410638000	-0.106233000
H	-6.692683000	-2.192384000	0.588208000
C	-5.436545000	-1.551430000	-1.169541000
H	-4.938618000	-2.477238000	-1.456191000
Fe	-0.001870000	-1.157175000	0.007272000
C	1.800076000	-0.450355000	0.908426000
C	1.790738000	-1.892611000	0.819574000
H	2.489878000	-2.514562000	0.264817000
C	0.710635000	-2.386701000	1.606754000
H	0.443332000	-3.436228000	1.737832000
C	0.036817000	-1.272459000	2.183486000
H	-0.842500000	-1.326104000	2.826587000
C	0.682037000	-0.087375000	1.747510000
H	0.402906000	0.931764000	2.011241000
C	-1.793679000	-0.423045000	-0.914847000
C	-0.640735000	-0.033514000	-1.695235000
H	-0.347379000	0.992992000	-1.909184000
C	0.004186000	-1.208067000	-2.164365000
H	0.902086000	-1.247502000	-2.782052000
C	-0.704272000	-2.335901000	-1.662912000
H	-0.443823000	-3.382684000	-1.826571000
C	-1.800852000	-1.862397000	-0.891413000
H	-2.521178000	-2.500506000	-0.383843000
C	3.225795000	2.925246000	0.416054000
H	3.164635000	3.157858000	-0.657846000
H	4.263460000	2.675685000	0.677971000
C	2.661022000	4.032654000	1.271962000
H	3.250745000	4.946729000	1.101619000
H	2.719298000	3.788502000	2.342928000
H	1.617146000	4.254440000	1.005210000
C	-3.248620000	2.933563000	-0.387877000
H	-3.177036000	3.163623000	0.685970000
H	-4.286982000	2.675215000	-0.638079000
C	-2.704803000	4.048996000	-1.247156000
H	-3.301311000	4.956833000	-1.067425000
H	-2.772957000	3.806872000	-2.317999000
H	-1.660041000	4.280197000	-0.992119000

Table S2. DFT-calculated *g*-tensors and hyperfine coupling parameters (hseh1pbe functional).

	6-311+g(d,p), DCM	**6-311+g(d,p)**	**6-311g(d,p)**	**SDD**
ge	2.0023193	2.0023193	2.0023193	2.0023193
xx shift	-4632.9	-5018	-4510.8	-2849.6
yy shift	31090.6	31140	33090.8	9549.2
zz shift	149600.2	151317.5	148546.9	57350.2
gxx calc	1.998	1.997	1.998	1.999
gyy calc	2.033	2.033	2.035	2.012
gzz calc	2.152	2.154	2.151	2.060
Mulliken spin density (Mn)	1.171117	1.085881	1.137988	1.288229
Isotr. Fermi CC (Mn)	-40.28306	-41.32886	-40.06647	-0.00977
Spin-dipole C (Mn) XX	0.572054	0.136272	0.001135	0.15867
Spin-dipole C (Mn) YY	0.243094	0.851704	0.956335	0.761654
Spin-dipole C (Mn) ZZ	-0.815148	-0.987977	-0.95747	-0.920324
Spin-dipole C (Mn) XY	-0.55689	-0.1361	-0.072735	-0.097623
Spin-dipole C (Mn) XZ	-0.754444	-1.055717	-1.03027	-1.062678
Spin-dipole C (Mn) YZ	-0.62088	-0.193459	-0.205451	-0.234293
Anis spin-dipole Baa (Mn)	-71.104	-77.409	-76.83	-75.293
Anis spin-dipole Bbb (Mn)	22.278	36.133	30.636	35.728
Anis spin-dipole Bcc (Mn)	48.826	41.276	46.194	39.565
Mulliken spin density (Fe)	-0.012732	-0.013773	-0.007966	-0.028687
Isotr. Fermi CC (Fe)	-0.06605	-0.04315	-0.0399	0.00004
Anis spin-dipole Baa (Fe)	-0.166	-0.164	-0.176	-0.752
Anis spin-dipole Bbb (Fe)	0.047	0.005	-0.001	-0.227
Anis spin-dipole Bcc (Fe)	0.119	0.159	0.177	0.979
Mn 4s	0.357	0.353	0.346	0.318
Mn 4px	0.348	0.329	0.021	0.317
Mn 4py	0.356	0.342	0.024	0.324
Mn 4pz	0.369	0.371	0.024	0.359
Mn 3dxy	1.318	1.330	1.246	1.357
Mn 3dxz	1.468	1.475	1.339	1.435
Mn 3dyz	1.457	1.188	1.094	1.205
Mn 3dx2-y2	1.095	1.174	1.046	1.144
Mn 3dz2	1.314	1.428	1.263	1.434
Valence e sum	8.082	7.990	6.404	7.895
3d e sum	6.652	6.594	5.989	6.576

Table S3. Cartesian coordinates and thermochemical parameters for compound **3a** calculated at the hseh1pbe/6-311+g(d,p) level of theory in a CH_2Cl_2 solvent continuum.

Center Number	Atomic Number	Atomic Type	Coordinates (Angstroms) X	Y	Z
1	6	0	2.269801	-1.342937	-1.931927
2	6	0	1.818794	-2.228068	-0.914004
3	6	0	0.739172	-1.608997	-0.243105
4	6	0	0.496402	-0.319759	-0.832600
5	6	0	1.483368	-0.167526	-1.881120
6	1	0	3.095944	-1.515870	-2.607073
7	1	0	2.254047	-3.185530	-0.666250
8	1	0	0.205851	-2.010121	0.603476
9	1	0	1.595642	0.671965	-2.547804
10	26	0	2.411764	-0.451753	-0.080116
11	6	0	2.714977	0.973251	1.370614
12	6	0	2.835648	-0.332211	1.922041
13	6	0	3.684934	1.108971	0.336935
14	1	0	1.991233	1.718380	1.670242
15	6	0	3.882001	-1.003973	1.230367
16	1	0	2.217659	-0.748684	2.704355
17	6	0	4.404757	-0.115753	0.249356
18	1	0	3.841986	1.980765	-0.282549
19	1	0	4.196601	-2.024971	1.392850
20	1	0	5.190082	-0.341444	-0.457911
21	6	0	-0.637495	0.536976	-0.451669
22	8	0	-0.559198	1.838717	-0.665129
23	6	0	0.579085	2.587477	-1.152572
24	1	0	0.567575	2.537495	-2.244614
25	1	0	1.497602	2.132505	-0.781863
26	6	0	0.414713	4.008337	-0.676628
27	1	0	0.425467	4.060003	0.414556
28	1	0	1.237933	4.617719	-1.058788
29	1	0	-0.523941	4.435533	-1.036758
30	25	0	-2.283440	-0.145873	0.243196
31	6	0	-4.288435	-0.832389	-0.123874
32	6	0	-3.681104	-0.461887	-1.361445
33	6	0	-3.532515	-1.887733	0.432219
34	1	0	-5.163780	-0.375291	0.314933
35	6	0	-2.560428	-1.308758	-1.561629
36	1	0	-4.020916	0.315119	-2.030685
37	6	0	-2.464089	-2.193821	-0.463058
38	1	0	-3.733671	-2.384050	1.371028
39	1	0	-1.886367	-1.272652	-2.405758
40	1	0	-1.730802	-2.975336	-0.335391
41	6	0	-2.863502	1.464234	0.665138
42	8	0	-3.314823	2.490894	0.952538
43	6	0	-1.535371	-0.355758	1.831624
44	8	0	-1.056264	-0.499760	2.877483

Zero-point correction=	0.340648 (Hartree/Particle)
Thermal correction to Energy=	0.364000
Thermal correction to Enthalpy=	0.364945
Thermal correction to Gibbs Free Energy=	0.285473
Sum of electronic and zero-point Energies=	-3412.338009
Sum of electronic and thermal Energies=	-3412.314657
Sum of electronic and thermal Enthalpies=	-3412.313712
Sum of electronic and thermal Free Energies=	-3412.393184

Table S4. Cartesian coordinates and thermochemical parameters for compound **3a**$^{\bullet+}$ calculated at the hseh1pbe/6-311+g(d,p) level of theory in a CH_2Cl_2 solvent continuum.

Center Number	Atomic Number	Atomic Type	Coordinates (Angstroms) X	Y	Z
1	6	0	2.577714	-0.516127	-2.194689
2	6	0	2.049676	-1.723640	-1.660001
3	6	0	0.854762	-1.421683	-0.981278
4	6	0	0.608968	0.002413	-1.081936
5	6	0	1.727474	0.550200	-1.838528
6	1	0	3.502835	-0.417380	-2.743961
7	1	0	2.507211	-2.699764	-1.727092
8	1	0	0.232386	-2.134310	-0.463478
9	1	0	1.892102	1.575532	-2.120324
10	26	0	2.382407	-0.355558	-0.142058
11	6	0	2.400099	0.440035	1.756359
12	6	0	2.613653	-0.965078	1.806232
13	6	0	3.430556	1.019338	0.964395
14	1	0	1.576047	0.971710	2.211652
15	6	0	3.781813	-1.254843	1.047313
16	1	0	1.985795	-1.686064	2.308528
17	6	0	4.285845	-0.030772	0.527368
18	1	0	3.536845	2.067106	0.721854
19	1	0	4.192328	-2.237336	0.864128
20	1	0	5.144414	0.076982	-0.119667
21	6	0	-0.525399	0.620930	-0.452327
22	8	0	-0.681612	1.907752	-0.354191
23	6	0	0.270771	2.935915	-0.762312
24	1	0	0.307277	2.938601	-1.853014
25	1	0	1.246344	2.665182	-0.353233
26	6	0	-0.233808	4.243600	-0.217615
27	1	0	-0.286708	4.221463	0.872718
28	1	0	0.453697	5.040133	-0.512090
29	1	0	-1.221909	4.479772	-0.617520
30	25	0	-2.156273	-0.305218	0.184386
31	6	0	-4.306553	-0.581777	-0.127563
32	6	0	-3.749990	0.240508	-1.147266
33	6	0	-3.674059	-1.839794	-0.179253
34	1	0	-5.063057	-0.282616	0.584220
35	6	0	-2.774366	-0.523812	-1.837870
36	1	0	-4.023874	1.265013	-1.354172
37	6	0	-2.715344	-1.808919	-1.229898
38	1	0	-3.865445	-2.673359	0.481259
39	1	0	-2.185896	-0.193072	-2.681443
40	1	0	-2.077676	-2.628062	-1.528826
41	6	0	-2.465826	0.881766	1.570158
42	8	0	-2.642378	1.611227	2.422684
43	6	0	-1.307223	-1.306144	1.449955
44	8	0	-0.798638	-1.924887	2.262367

Zero-point correction=	0.341128 (Hartree/Particle)
Thermal correction to Energy=	0.364950
Thermal correction to Enthalpy=	0.365894
Thermal correction to Gibbs Free Energy=	0.285007
Sum of electronic and zero-point Energies=	-3412.170255
Sum of electronic and thermal Energies=	-3412.146433
Sum of electronic and thermal Enthalpies=	-3412.145489
Sum of electronic and thermal Free Energies=	-3412.226376

Table S5. Cartesian coordinates and thermochemical parameters for compound **3a** calculated at the hseh1pbe/6-311+g(d,p) level of theory in vacuo.

Center Number	Atomic Number	Atomic Type	Coordinates (Angstroms) X	Y	Z
1	6	0	2.323159	-1.291384	-1.974919
2	6	0	1.849441	-2.210672	-0.999405
3	6	0	0.742155	-1.622261	-0.345409
4	6	0	0.502165	-0.319639	-0.903860
5	6	0	1.518230	-0.128458	-1.916234
6	1	0	3.171714	-1.435350	-2.628664
7	1	0	2.286267	-3.171308	-0.767262
8	1	0	0.190522	-2.046762	0.477216
9	1	0	1.643141	0.731377	-2.553713
10	26	0	2.391894	-0.454515	-0.093304
11	6	0	2.619513	0.975384	1.365160
12	6	0	2.674090	-0.326466	1.932549
13	6	0	3.661766	1.084889	0.402254
14	1	0	1.887799	1.732720	1.608967
15	6	0	3.754460	-1.022024	1.323225
16	1	0	1.985352	-0.721170	2.665476
17	6	0	4.362912	-0.152996	0.375186
18	1	0	3.880854	1.949390	-0.208589
19	1	0	4.039018	-2.046160	1.517678
20	1	0	5.195240	-0.397610	-0.268998
21	6	0	-0.634874	0.526389	-0.495865
22	8	0	-0.553239	1.837775	-0.687793
23	6	0	0.573416	2.599423	-1.160053
24	1	0	0.567160	2.571797	-2.254600
25	1	0	1.499863	2.151055	-0.798481
26	6	0	0.391154	4.011332	-0.660042
27	1	0	0.398543	4.042437	0.431910
28	1	0	1.201805	4.644840	-1.030907
29	1	0	-0.558309	4.425766	-1.005443
30	25	0	-2.250313	-0.151509	0.235941
31	6	0	-4.273344	-0.831127	-0.040993
32	6	0	-3.705915	-0.495847	-1.306308
33	6	0	-3.508265	-1.878754	0.513823
34	1	0	-5.126036	-0.352492	0.418436
35	6	0	-2.600936	-1.358541	-1.525014
36	1	0	-4.060536	0.270261	-1.980026
37	6	0	-2.475523	-2.217789	-0.410323
38	1	0	-3.679604	-2.347734	1.472209
39	1	0	-1.956711	-1.351466	-2.392775
40	1	0	-1.751985	-3.009950	-0.294424
41	6	0	-2.822668	1.477315	0.643066
42	8	0	-3.266139	2.505827	0.913838
43	6	0	-1.441685	-0.331840	1.805611
44	8	0	-0.905753	-0.463120	2.822043

Zero-point correction=	0.341305 (Hartree/Particle)
Thermal correction to Energy=	0.364496
Thermal correction to Enthalpy=	0.365440
Thermal correction to Gibbs Free Energy=	0.287726
Sum of electronic and zero-point Energies=	-3412.326872
Sum of electronic and thermal Energies=	-3412.303681
Sum of electronic and thermal Enthalpies=	-3412.302737
Sum of electronic and thermal Free Energies=	-3412.380451

Table S6. Cartesian coordinates and thermochemical parameters for compound **3a**$^{\bullet+}$ calculated at the hseh1pbe/6-311+g(d,p) level of theory in vacuo.

Center Number	Atomic Number	Atomic Type	Coordinates (Angstroms) X	Y	Z
1	6	0	2.576464	-0.484132	-2.201900
2	6	0	2.054241	-1.697723	-1.676938
3	6	0	0.861227	-1.406503	-0.991278
4	6	0	0.606286	0.017997	-1.081271
5	6	0	1.725005	0.575929	-1.833034
6	1	0	3.496543	-0.379132	-2.758626
7	1	0	2.513577	-2.671944	-1.759455
8	1	0	0.242217	-2.124143	-0.476333
9	1	0	1.883980	1.603159	-2.111249
10	26	0	2.385170	-0.342647	-0.144988
11	6	0	2.423391	0.418080	1.771819
12	6	0	2.635194	-0.986799	1.793849
13	6	0	3.446472	1.011016	0.981982
14	1	0	1.612471	0.943461	2.257171
15	6	0	3.796121	-1.262377	1.021166
16	1	0	2.017086	-1.715490	2.297069
17	6	0	4.296534	-0.030736	0.519636
18	1	0	3.563826	2.064419	0.771289
19	1	0	4.211284	-2.240602	0.826083
20	1	0	5.156830	0.089242	-0.122918
21	6	0	-0.532547	0.623078	-0.453450
22	8	0	-0.705393	1.911737	-0.359102
23	6	0	0.236030	2.951697	-0.761210
24	1	0	0.277963	2.957184	-1.852682
25	1	0	1.214536	2.688027	-0.352869
26	6	0	-0.283008	4.254325	-0.216776
27	1	0	-0.338571	4.233823	0.873393
28	1	0	0.393291	5.061521	-0.508809
29	1	0	-1.273229	4.481339	-0.616381
30	25	0	-2.160837	-0.309369	0.188419
31	6	0	-4.314008	-0.598961	-0.130579
32	6	0	-3.755708	0.201811	-1.164938
33	6	0	-3.676296	-1.854723	-0.148723
34	1	0	-5.081280	-0.289200	0.565578
35	6	0	-2.773073	-0.573349	-1.831836
36	1	0	-4.039253	1.217327	-1.402122
37	6	0	-2.711110	-1.843495	-1.194303
38	1	0	-3.876103	-2.676714	0.524182
39	1	0	-2.185562	-0.262613	-2.683840
40	1	0	-2.076261	-2.669796	-1.479839
41	6	0	-2.479688	0.880476	1.578964
42	8	0	-2.658010	1.609348	2.429048
43	6	0	-1.277901	-1.295333	1.445138
44	8	0	-0.740173	-1.904648	2.244011

Zero-point correction=	0.341322 (Hartree/Particle)
Thermal correction to Energy=	0.365230
Thermal correction to Enthalpy=	0.366175
Thermal correction to Gibbs Free Energy=	0.284525
Sum of electronic and zero-point Energies=	-3412.114934
Sum of electronic and thermal Energies=	-3412.091025
Sum of electronic and thermal Enthalpies=	-3412.090081
Sum of electronic and thermal Free Energies=	-3412.171731

Table S7. Cartesian coordinates and thermochemical parameters for compound **3a** calculated at the hseh1pbe/6-311g(d,p) level of theory in vacuo.

Center Number	Atomic Number	Atomic Type	Coordinates (Angstroms) X	Y	Z
1	6	0	2.334707	-1.228571	-1.999101
2	6	0	1.859492	-2.175781	-1.053311
3	6	0	0.745916	-1.611204	-0.391072
4	6	0	0.505389	-0.293187	-0.911712
5	6	0	1.523498	-0.072795	-1.915366
6	1	0	3.188124	-1.350175	-2.650814
7	1	0	2.298564	-3.140630	-0.845031
8	1	0	0.193513	-2.064074	0.415561
9	1	0	1.648043	0.802278	-2.531362
10	26	0	2.381745	-0.444914	-0.100192
11	6	0	2.614399	0.987398	1.347700
12	6	0	2.609487	-0.309733	1.926699
13	6	0	3.682936	1.053393	0.411445
14	1	0	1.903499	1.771103	1.567937
15	6	0	3.681215	-1.045595	1.352816
16	1	0	1.887116	-0.674779	2.642302
17	6	0	4.342431	-0.206872	0.414077
18	1	0	3.944622	1.903754	-0.202233
19	1	0	3.926614	-2.076204	1.564638
20	1	0	5.183351	-0.484935	-0.204595
21	6	0	-0.638607	0.534803	-0.487854
22	8	0	-0.567974	1.850013	-0.666806
23	6	0	0.551477	2.625622	-1.128846
24	1	0	0.541687	2.621987	-2.223683
25	1	0	1.481674	2.175888	-0.779914
26	6	0	0.361986	4.024308	-0.596258
27	1	0	0.373800	4.027932	0.495893
28	1	0	1.163995	4.674778	-0.955568
29	1	0	-0.594069	4.435816	-0.925724
30	25	0	-2.238033	-0.159882	0.239079
31	6	0	-4.261270	-0.798447	-0.069971
32	6	0	-3.674122	-0.443405	-1.320295
33	6	0	-3.518619	-1.867571	0.471380
34	1	0	-5.112377	-0.316982	0.389163
35	6	0	-2.580422	-1.318408	-1.544554
36	1	0	-4.012172	0.338957	-1.983147
37	6	0	-2.479025	-2.201236	-0.447549
38	1	0	-3.708666	-2.355270	1.416592
39	1	0	-1.924514	-1.301881	-2.403172
40	1	0	-1.768597	-3.006391	-0.341591
41	6	0	-2.796840	1.454631	0.706889
42	8	0	-3.231384	2.478441	1.003582
43	6	0	-1.412694	-0.428338	1.781526
44	8	0	-0.862736	-0.639756	2.776087

Zero-point correction=	0.341951 (Hartree/Particle)
Thermal correction to Energy=	0.365007
Thermal correction to Enthalpy=	0.365952
Thermal correction to Gibbs Free Energy=	0.288723
Sum of electronic and zero-point Energies=	-3412.296163
Sum of electronic and thermal Energies=	-3412.273107
Sum of electronic and thermal Enthalpies=	-3412.272162
Sum of electronic and thermal Free Energies=	-3412.349391

Table S8. Cartesian coordinates and thermochemical parameters for compound **3a**$^{\bullet+}$ calculated at the hseh1pbe/6-311g(d,p) level of theory in vacuo.

Center Number	Atomic Number	Atomic Type	Coordinates (Angstroms) X	Y	Z
1	6	0	2.609134	-0.351138	-2.199685
2	6	0	2.093995	-1.593383	-1.742504
3	6	0	0.891180	-1.348532	-1.057396
4	6	0	0.619579	0.075318	-1.083736
5	6	0	1.742302	0.680625	-1.790159
6	1	0	3.534438	-0.209515	-2.739075
7	1	0	2.563932	-2.557703	-1.868097
8	1	0	0.275471	-2.098792	-0.587653
9	1	0	1.893954	1.721235	-2.017381
10	26	0	2.386743	-0.314720	-0.149592
11	6	0	2.331946	0.240351	1.828586
12	6	0	2.677483	-1.130501	1.711332
13	6	0	3.300714	1.006341	1.123160
14	1	0	1.470614	0.632782	2.350752
15	6	0	3.865252	-1.214131	0.935600
16	1	0	2.125079	-1.961255	2.124200
17	6	0	4.250502	0.104064	0.574105
18	1	0	3.321609	2.082517	1.028980
19	1	0	4.375470	-2.123070	0.651847
20	1	0	5.101627	0.371775	-0.035003
21	6	0	-0.537125	0.629550	-0.444516
22	8	0	-0.748962	1.910306	-0.318669
23	6	0	0.149352	2.990858	-0.711576
24	1	0	0.201638	3.000557	-1.802505
25	1	0	1.134067	2.770675	-0.293868
26	6	0	-0.431804	4.265986	-0.165948
27	1	0	-0.501665	4.231953	0.922864
28	1	0	0.211901	5.104713	-0.441190
29	1	0	-1.425532	4.452076	-0.577266
30	25	0	-2.142661	-0.327344	0.183741
31	6	0	-4.285978	-0.617034	-0.168686
32	6	0	-3.710515	0.143713	-1.220255
33	6	0	-3.644461	-1.869697	-0.122035
34	1	0	-5.067411	-0.281202	0.499102
35	6	0	-2.714432	-0.652484	-1.837433
36	1	0	-3.990278	1.149220	-1.499971
37	6	0	-2.659887	-1.895950	-1.150527
38	1	0	-3.860753	-2.667712	0.573646
39	1	0	-2.108833	-0.370971	-2.686800
40	1	0	-2.025829	-2.734212	-1.399299
41	6	0	-2.508187	0.810921	1.600397
42	8	0	-2.726293	1.517136	2.459209
43	6	0	-1.202334	-1.306151	1.387296
44	8	0	-0.617066	-1.922333	2.146515

Zero-point correction=	0.341768 (Hartree/Particle)
Thermal correction to Energy=	0.365605
Thermal correction to Enthalpy=	0.366549
Thermal correction to Gibbs Free Energy=	0.285047
Sum of electronic and zero-point Energies=	-3412.084912
Sum of electronic and thermal Energies=	-3412.061075
Sum of electronic and thermal Enthalpies=	-3412.060131
Sum of electronic and thermal Free Energies=	-3412.141633

Table S9. Cartesian coordinates and thermochemical parameters for compound **3a** calculated at the hseh1pbe/SDD level of theory in vacuo.

Center Number	Atomic Number	Atomic Type	Coordinates (Angstroms) X	Y	Z
1	6	0	2.343439	-1.290287	-2.016433
2	6	0	1.858920	-2.235336	-1.047149
3	6	0	0.731943	-1.654684	-0.390243
4	6	0	0.491045	-0.334537	-0.939805
5	6	0	1.523806	-0.120537	-1.948152
6	1	0	3.190455	-1.427462	-2.673167
7	1	0	2.288461	-3.203344	-0.833623
8	1	0	0.165624	-2.093669	0.414539
9	1	0	1.639844	0.744266	-2.580769
10	26	0	2.389687	-0.468116	-0.098758
11	6	0	2.595648	0.970238	1.388601
12	6	0	2.639683	-0.348690	1.955885
13	6	0	3.666218	1.084998	0.434648
14	1	0	1.867239	1.730231	1.633492
15	6	0	3.741808	-1.049795	1.355627
16	1	0	1.943715	-0.739923	2.683730
17	6	0	4.374438	-0.166592	0.413033
18	1	0	3.904663	1.955946	-0.159597
19	1	0	4.029883	-2.071289	1.559002
20	1	0	5.225425	-0.404692	-0.208985
21	6	0	-0.647123	0.510259	-0.524023
22	8	0	-0.555103	1.857120	-0.717317
23	6	0	0.600535	2.653763	-1.172293
24	1	0	0.600270	2.647998	-2.269167
25	1	0	1.525994	2.202667	-0.804370
26	6	0	0.385985	4.056224	-0.634618
27	1	0	0.383799	4.057910	0.459962
28	1	0	1.185421	4.720717	-0.984382
29	1	0	-0.574151	4.455638	-0.974447
30	25	0	-2.240963	-0.135433	0.235286
31	6	0	-4.300538	-0.771772	-0.136778
32	6	0	-3.603201	-0.644958	-1.390226
33	6	0	-3.645039	-1.773877	0.635503
34	1	0	-5.161847	-0.195551	0.169974
35	6	0	-2.527113	-1.594464	-1.385932
36	1	0	-3.861907	0.024529	-2.197605
37	6	0	-2.549159	-2.293812	-0.144346
38	1	0	-3.930503	-2.100506	1.625100
39	1	0	-1.817729	-1.748679	-2.186176
40	1	0	-1.891770	-3.099092	0.148275
41	6	0	-2.816598	1.493581	0.554254
42	8	0	-3.276234	2.560129	0.782564
43	6	0	-1.425228	-0.245495	1.785322
44	8	0	-0.850848	-0.337776	2.823067

Zero-point correction=	0.343992 (Hartree/Particle)
Thermal correction to Energy=	0.367325
Thermal correction to Enthalpy=	0.368269
Thermal correction to Gibbs Free Energy=	0.289991
Sum of electronic and zero-point Energies=	-1225.815962
Sum of electronic and thermal Energies=	-1225.792629
Sum of electronic and thermal Enthalpies=	-1225.791684
Sum of electronic and thermal Free Energies=	-1225.869963

Table S10. Cartesian coordinates and thermochemical parameters for compound **3a**$^{\bullet+}$ calculated at the hseh1pbe/SDD level of theory in vacuo.

Center Number	Atomic Number	Atomic Type	Coordinates (Angstroms) X	Y	Z
1	6	0	2.608961	-0.352130	-2.240337
2	6	0	2.099814	-1.615337	-1.777682
3	6	0	0.887497	-1.379279	-1.077528
4	6	0	0.602541	0.056344	-1.100099
5	6	0	1.726186	0.680349	-1.817872
6	1	0	3.524199	-0.204332	-2.794766
7	1	0	2.571005	-2.576619	-1.920289
8	1	0	0.271962	-2.132101	-0.611028
9	1	0	1.862509	1.723053	-2.046634
10	26	0	2.400213	-0.319757	-0.153709
11	6	0	2.404482	0.354761	1.819550
12	6	0	2.644485	-1.060494	1.775376
13	6	0	3.435314	1.010708	1.062509
14	1	0	1.585763	0.841365	2.331442
15	6	0	3.831987	-1.279813	0.996503
16	1	0	2.038520	-1.820818	2.244886
17	6	0	4.320026	-0.002779	0.555991
18	1	0	3.542373	2.075730	0.914595
19	1	0	4.275419	-2.238889	0.770806
20	1	0	5.193030	0.164807	-0.058244
21	6	0	-0.553113	0.614725	-0.457505
22	8	0	-0.769371	1.930379	-0.336909
23	6	0	0.126266	3.055002	-0.747555
24	1	0	0.174635	3.055667	-1.841287
25	1	0	1.115849	2.861069	-0.320598
26	6	0	-0.499700	4.320752	-0.206008
27	1	0	-0.568620	4.293349	0.885259
28	1	0	0.116364	5.181927	-0.488222
29	1	0	-1.502132	4.471858	-0.616557
30	25	0	-2.138174	-0.339345	0.202590
31	6	0	-4.317636	-0.670536	-0.127317
32	6	0	-3.754043	0.079733	-1.215635
33	6	0	-3.658796	-1.932381	-0.063860
34	1	0	-5.103579	-0.332267	0.533777
35	6	0	-2.748370	-0.730934	-1.834513
36	1	0	-4.051424	1.073258	-1.520061
37	6	0	-2.676586	-1.972769	-1.114238
38	1	0	-3.866438	-2.721937	0.644181
39	1	0	-2.163473	-0.468779	-2.704302
40	1	0	-2.046911	-2.815965	-1.358606
41	6	0	-2.502427	0.859890	1.546666
42	8	0	-2.707061	1.632472	2.393748
43	6	0	-1.204942	-1.260999	1.436242
44	8	0	-0.592557	-1.848093	2.244562

Zero-point correction=	0.343892 (Hartree/Particle)
Thermal correction to Energy=	0.367890
Thermal correction to Enthalpy=	0.368835
Thermal correction to Gibbs Free Energy=	0.287102
Sum of electronic and zero-point Energies=	-1225.601774
Sum of electronic and thermal Energies=	-1225.577776
Sum of electronic and thermal Enthalpies=	-1225.576831
Sum of electronic and thermal Free Energies=	-1225.658564

References

[1] a) B. Van der Westhuizen, P. J. Swarts, I. Strydom, D. C. Liles, I. Fernández, J. C. Swarts, D. I. Bezuidenhout, *Dalton Trans.* **2013**, *42*, 5367-5378; b) B. Van der Westhuizen, P. J. Swarts, L. M. van Jaarsveld, D. C. Liles, U. Siegert, J. C. Swarts, I. Fernández, D. I. Bezuidenhout, *Inorg. Chem.* **2013**, *52*, 6674-6684.

[2] D. I. Bezuidenhout, I. Fernández, B. Van der Westhuizen,, P. J. Swarts, J. C. Swarts, *Organometallics,* **2013**, *32*, 7334-7344.